

Journal Pre-proofs

4-(4-Chlorophenyl)thiazol-2-amines as pioneers of potential neurodegenerative therapeutics with anti-inflammatory properties based on dual DNase I and 5-LO inhibition

Andrija Smelcerovic, Aleksandra Zivkovic, Budimir S. Ilic, Ana Kolarevic, Bettina Hofmann, Dieter Steinhilber, Holger Stark

PII: S0045-2068(19)31094-6
DOI: <https://doi.org/10.1016/j.bioorg.2019.103528>
Reference: YBIOO 103528

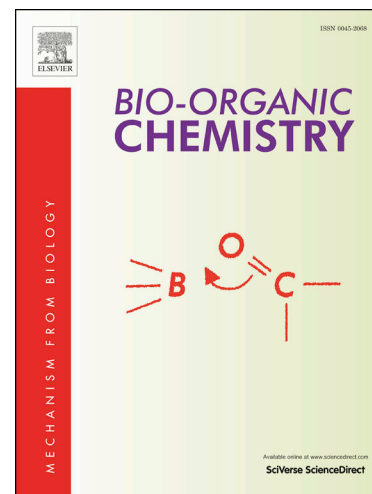
To appear in: *Bioorganic Chemistry*

Received Date: 9 July 2019
Revised Date: 16 December 2019
Accepted Date: 19 December 2019

Please cite this article as: A. Smelcerovic, A. Zivkovic, B.S. Ilic, A. Kolarevic, B. Hofmann, D. Steinhilber, H. Stark, 4-(4-Chlorophenyl)thiazol-2-amines as pioneers of potential neurodegenerative therapeutics with anti-inflammatory properties based on dual DNase I and 5-LO inhibition, *Bioorganic Chemistry* (2019), doi: <https://doi.org/10.1016/j.bioorg.2019.103528>

This is a PDF file of an article that has undergone enhancements after acceptance, such as the addition of a cover page and metadata, and formatting for readability, but it is not yet the definitive version of record. This version will undergo additional copyediting, typesetting and review before it is published in its final form, but we are providing this version to give early visibility of the article. Please note that, during the production process, errors may be discovered which could affect the content, and all legal disclaimers that apply to the journal pertain.

© 2019 Published by Elsevier Inc.



therapeutics with anti-inflammatory properties based on dual DNase I and 5-LO inhibition

Andrija Smelcerovic^{a,*}, Aleksandra Zivkovic^b, Budimir S. Ilic^a, Ana Kolarevic^c, Bettina Hofmann^d, Dieter Steinhilber^d, Holger Stark^{b,*}

^a *Department of Chemistry, Faculty of Medicine, University of Nis, Bulevar Dr Zorana Djindjica 81, 18000 Nis, Serbia*

^b *Institute of Pharmaceutical and Medicinal Chemistry, Heinrich Heine University Düsseldorf, Düsseldorf, Germany*

^c *Department of Pharmacy, Faculty of Medicine, University of Nis, Bulevar Dr Zorana Djindjica 81, 18000 Nis, Serbia*

^d *Institute of Pharmaceutical Chemistry, Goethe University Frankfurt, Frankfurt/Main, Germany*

*Corresponding authors

E-mail addresses: a.smelcerovic@yahoo.com (or andrija.smelcerovic@medfak.ni.ac.rs) (A. Smelcerovic), stark@hhu.de (H. Stark)

ABSTRACT

Eleven new 4-(4-chlorophenyl)thiazol-2-amines were synthesized and, together with nine known derivatives, evaluated *in vitro* for inhibitory properties towards bovine pancreatic DNase I. Three compounds (**18-20**) inhibited DNase I with IC₅₀ values below 100 μM, with compound **19** being the most potent (IC₅₀ = 79.79 μM). Crystal violet, used as a positive control in the absence of a "golden standard", exhibited almost 5-fold weaker DNase I inhibition. Pharma/E-State RQSAR models clarified critical structural fragments relevant for DNase I inhibition. Molecular docking and molecular dynamics simulation defined the 4-(4-chlorophenyl)thiazol-2-amines interactions with the most important catalytic residues of DNase I. Ligand-based pharmacophore modeling and virtual screening confirmed the chemical features of 4-(4-chlorophenyl)thiazol-2-amines required for DNase I inhibition and proved the absence of structurally similar molecules in available databases. Compounds **18-20** have been shown as very potent 5-LO inhibitors with nanomolar IC₅₀ values obtained in cell-free assay, with compound **20** being the most potent (IC₅₀ = 50 nM).

Molecular docking and molecular dynamics simulations into the binding site of 5-LO enzyme allowed us to clarify the binding mode of these dual DNase I/5-LO inhibitors. It was shown that compounds **18-20** uniquely show interactions with histidine residues in the catalytic site of DNase I and 5-LO enzyme. In the absence of potent organic DNase I inhibitors, compounds **18-20** represent a good starting point for the development of novel Alzheimer's therapeutics based on dual 5-LO and DNase I inhibition, which also have anti-inflammatory properties.

KEYWORDS

DNase I, 5-Lipoxygenase, Inhibition, Molecular dynamics, Pharmacophore modeling, Alzheimer

1. INTRODUCTION

It is widely known that the deoxyribonucleic acid (DNA) is one of the key macromolecules necessary for the continuity of life. Bovine pancreatic deoxyribonuclease I (DNase I) [EC 3.1.21.1] is one of the best characterized mammal endonucleases that breaks both single-stranded and double-stranded DNA producing 3'-OH/5'-P ends [1,2]. To exert its full activity, DNase I requires the presence of both Mg^{2+} and Ca^{2+} and optimal pH between 7.0 and 8.0 [3]. DNase I is one of the major nucleases involved in DNA degradation during apoptosis [2,4–8], acting as both cell-autonomous and waste-management nuclease [2,7], and thus might have a crucial role in the development of many disease conditions caused by excessive cell death (Table 1). Inhibition of DNase I is an important mechanism for protecting DNA from premature degradation during cell damage [9]. DNase I inhibitors represent an attractive potential target for the design of alternative strategies for the prevention and/or therapy of numerous pathological conditions caused by elevated DNase I levels and/or excessive apoptosis (Table 1).

Table 1

Potential therapeutic applications of DNase I inhibitors.

Conditions caused by excessive apoptosis	Reference
Autoimmune disorders <i>AIDS</i>	[7,10]
Neurodegenerative disorders <i>Alzheimer's disease</i> <i>Parkinson's disease</i> <i>Huntington's disease</i> <i>Amyotrophic lateral sclerosis</i> <i>Retinitis pigmentosa</i> <i>Spinal muscular atrophy</i> <i>Cerebellar degeneration</i>	[7,10–13]
Graft-versus-host disease	[7]
Ischemic disorders <i>Myocardial ischaemia</i> <i>Myocardial infarction</i> <i>Stroke</i>	[7,10,13–15]
Acute fatty degeneration of the liver	[16]
Conditions followed by elevated DNase I levels	
Myocardial dysfunction among elderly	[17]
Idiopathic dilated cardiomyopathy	[18]
Type 2 diabetes	[19]
Cisplatin-induced nephrotoxicity	[20–22]
Gamma-induced damage	[23]
Acetaminophen-induced hepatocellular necrosis	[24]

2-Aminothiazole and its derivatives have been used as precursors for the synthesis of many compounds with various biological activities [25], such as anticancer, anticonvulsant, antidiabetic, antihypertensive, anti-inflammatory, antimicrobial, antioxidant, antitumor, and antiviral. Some of the drugs containing 2-aminothiazole core are already in the market. 2-Aminothiazole scaffold is an excellent pharmacophore for the development of many more biologically active derivatives [26].

As the number of known organic DNase I inhibitors, especially those with potential therapeutic applications, is relatively small [27], continuing our research on finding novel ones [28–33], in the present study a series of twenty 4-(4-chlorophenyl)thiazol-2-amines (Table 2) was evaluated for inhibitory activity against bovine pancreatic DNase I *in vitro*. Some of them were previously synthesized and evaluated as ligands for varying targets: as inhibitors of eicosanoid metabolism (**1**) [34], sphingosine kinase inhibitors (**1**, **2**, **7**, **15-17**) [35], and 5-lipoxygenase (5-LO) inhibitors (**1**, **14**, **17**, **18**, **20**) [36].

Having in mind that our studied molecules were built on a similar scaffold, by attaching different groups at one or more points on the 4-(4-chlorophenyl)thiazol-2-amine, we wanted to examine DNase I inhibitory properties of the 4-(4-chlorophenyl)thiazol-2-amines as a function of the groups at the various attachment points. In addition, we wanted to clarify DNase I inhibitory properties of 4-(4-chlorophenyl)thiazol-2-amines at the molecular level using molecular docking studies. Furthermore, the most active 4-(4-chlorophenyl)thiazol-2-amines were subjected to the molecular dynamics simulations, in order to further evaluate the stability of their binding to the active site of DNase I. Ligand-based pharmacophore modeling approach was performed in order to reveal and confirm the chemical features of 4-(4-chlorophenyl)thiazol-2-amines required for DNase I inhibition. Pharmacophore based virtual screening study was carried out using PubChem compound database to find novel/potent DNase I inhibitors with 4-(4-chlorophenyl)thiazol-2-amine moiety.

In order to perceive the multiple biological effects of the most potent DNase I inhibitors, an attempt was made to connect their DNase I inhibitory properties with previously reported [36] and new data on their 5-LO inhibitory properties, considering the importance of these enzymes in the development of neurodegenerative disorders in the elderly, such as is Alzheimer's disease. Molecular docking and molecular dynamics simulations into the binding site of 5-LO enzyme allowed us to clarify the binding mode of these novel dual DNase I/5-LO inhibitors. An *in silico* study of the physico-chemical, pharmacokinetic and toxicological properties of most potent DNase I inhibitors was also performed.

2. MATERIALS AND METHODS

2.1. Synthesis of 4-(4-chlorophenyl)thiazol-2-amines

All commercial chemicals were reagent grade and used as purchased by Sigma–Aldrich (Steinheim/Germany), ABCR (Karlsruhe/Germany), Acros Organics (Geel/Belgium), Alfa-Aesar (Karlsruhe/Germany) and Fluorochem (Derbyshire/UK) unless otherwise indicated. Only dried solvents were used. Reactions were monitored by thin-layer chromatography using silica gel 60 F254 aluminumbacked plate from Merck (Darmstadt/Germany) with detection using a UV lamp and ninhydrin. Column chromatography was performed on silica gel (SiO₂, 40–63 μm). Microwave-assisted synthesis was performed using a Biotage Initiator 2.0, 400 Watt microwave synthesizer (Biotage, Uppsala/Sweden). All products were characterized by ¹H NMR and ¹³C NMR. NMR spectra were recorded on a Bruker AV 250 (¹H: 250 MHz; ¹³C: 63 MHz) spectrometer (Bruker, Karlsruhe/Germany) and Bruker AV 400 (¹H: 400 MHz; ¹³C: 75 MHz) spectrometer (Bruker, Karlsruhe/Germany). Chemical shifts (δ) are reported in ppm relative to tetramethylsilane (TMS) as internal standard. Multiplicity: s = singlet, d = doublet, t = triplet, q = quartet, m = multiplet; coupling constants (J) are shown in hertz (Hz); number and assignment of protons. Mass spectra were obtained on VG Platform II (Fisons Instruments, Ipswich/UK) using electrospray ionization (ESI). Data are listed as mass number

[M+H]⁺ or [M-H]⁺. High resolution MS (HR-MS) were achieved on a LTO Orbitrap XL (Thermo Fisher Scientific, Waltham/USA). For final compounds the analyses were within ± 5 ppm of the theoretical values. The purity of the compounds was determined by elemental analysis (C, H, N, S) on a MicroCube instrument (Elementar, Hanau/Germany) and was within $\pm 0.4\%$ of the theoretical values for all final compounds, which corresponds to 95% purity.

Studied 4-(4-chlorophenyl)thiazol-2-amines were synthesized according to the general procedure for the synthesis of 2-aminothiazole derivatives [35]. The cyclic condensation of an α -bromoketone (1 eq.) and *N*-substituted thiourea (1 eq.) in anhydrous ethanol, stirring under microwave irradiation at 80°C for 30 min. The precipitating hydrobromide salts were collected and washed with water and cold ethanol. If needed, further purification was done after neutralization with saturated ammoniumhydroxide solution, stirring at room temperature, filtration of the precipitate and washing with cold ethanol. Column chromatography on silica gel (eluent: hexane/ethylacetate 2:1 or dichloromethane/methanol 9:1) afforded the titled compounds in variable yields.

N-(4-(4-Chlorophenyl)thiazol-2-yl)cinnamic acid amide (Compound 3; Table 2)

¹H-NMR (250 MHz, DMSO-d₆, δ): 12.58 (s, 1H, NH-C=O), 7.95 (d, J = 8.5, 2H, Cl-Ph-3-H, -5-H), 7.78 (d, 2H, Ph-2-H, -6-H), 7.65 (d, 2H, Cl-Ph-2-H, -6-H), 7.50 (m, 5H, Thiazol-5-H, Ph-3-H, -5-H, -4-H, C=O-CH=CH), 6.98 (d, J = 15.9, 1H, C=O-CH=CH); ¹³C-NMR (63 MHz, DMSO-d₆, δ): δ 163.48, 158.18, 147.85, 142.49, 134.26, 133.18, 132.29, 130.32, 129.10, 128.76, 128.01, 127.40, 119.52, 109.26; ESI-MS (m/z) 339.1 [M-H]⁺; CHN Calculated: C 63.43%, H 3.84%, N 8.22%, S 9.41%; Found: C 63.36%, H 3.80%, N 8.16%, S 9.64%; Yield: 25 %; Colourless crystals.

N-(4-(4-Chlorophenyl)thiazol-2-yl)benzamide (Compound 4; Table 2)

¹H-NMR (250 MHz, DMSO-d₆, δ): 12.84 (s, 1H, NH-C=O), 8.15 (d, J = 8.0, 2H, Ph-2-H, 6-H), 7.99 (d, J = 8.6, 1H, Cl-Ph-3-H, -5-H), 7.77 (s, 1H, Thiazol-5-H), 7.67 (t, 1H, Ph-4-H), 7.57 (t, 2H, Ph-3-H, -5-H), 7.52 (d, J = 8.7, 2H, Cl-Ph -2-H, -6-H); ¹³C-NMR (63 MHz, DMSO-d₆, δ): 165.30, 158.76, 147.97, 133.30, 132.66, 132.34, 131.96, 128.85, 128.60, 128.22, 127.52, 109.35; ESI-MS (m/z): 313.0 [M-H]⁺; CHN Calculated: C 61.05%, H 3.52%, N 8.90%, S 10.19%; Found: C 61.05%, H 3.60%, N 8.96%, S 10.26%; Yield: 66 %; Colourless crystals.

4-(4-Chlorophenyl)-5-methyl-*N*-(pyridin-2-yl)thiazol-2-amine (Compound 5; Table 2)

¹H-NMR (250 MHz, DMSO-d⁶, δ): 11.23 (s, 1H, -NH-), 8.28 (d, 1H, J = 5.0 Hz, py-6H), 7.72-7.65 (m, 3H, Ph-Cl-2H,6H, py-4H), 7.48 (d, 2H, J = 8.5 Hz, Ph-Cl-3H,5H), 7.05 (d, 1H, J = 8.5 Hz, py-3H), 6.90 (t, 1H, J = 5.2 Hz, py-5H), 2.45 (s, 3H, -CH₃); ¹³C-NMR (63 MHz, DMSO-d⁶, δ): 155.53, 151.64, 146.29, 142.29, 137.70, 134.14, 131.30, 129.38, 128.16, 119.22, 115.66, 110.46, 11.64; ESI-MS (m/z): 302.1 [M+H⁺]; CHN Calculated: C 59.70%, H 4.01%, N 13.92%, S 10.62%; Found: C 59.81%, H 3.95%, N 13.90%, S 10.54%; Yield: 14 %; White amorphous solid.

4-(4-Chlorophenyl)-N-(2-methoxypyridin-4-yl)-5-methylthiazol-2-amine (Compound **6**; Table 2)

¹H-NMR (250 MHz, DMSO-d⁶, δ) : 10.53 (s, 1H, -NH-), 7.96 (d, 1H, J = 5.7 Hz, pyridine-6H), 7.69 (d, 2H, J = 8.6 Hz, Ph-Cl-2H,6H), 7.53 (d, 2H, J = 8.6 Hz, Ph-Cl-3H,5H), 7.23 (sd, 1H, J = 1.7 Hz, pyridine-3H), 6.99 (dd, 1H, J = 5.8 Hz, 1.8 Hz, pyridine-5H), 3.80 (s, 3H, pyridine-CH₃), 2.45 (s, 3H, thiazole-CH₃); ¹³C-NMR (63 MHz, DMSO-d⁶, δ): 164.73, 158.11, 149.14, 146.95, 144.18, 133.55, 131.77, 129.52, 128.38, 118.97, 106.49, 95.40, 52.86, 11.81; ESI-MS (m/z) 330.0 [M+H⁺]; CHN Calculated: C 57.91%, H 4.25%, N 12.66%, S 9.66%; Found: C 57.85%, H 4.25%, N 12.55%, S 9.96%; Yield: 5 %; White solid.

4-(4-Chlorophenyl)-N-(2-methoxyphenyl)-5-methylthiazol-2-amin (Compound **8**; Table 2)

¹H-NMR (250 MHz, DMSO-d⁶, δ): 10.22 (s, 1H, -NH-), 7.98 (d, 1H, J = 7.8 Hz, 3H-Ph-OCH₃), 7.62 (d, 2H, J = 8.6 Hz, 2H,6H-Ph-Cl), 7.53 (d, 2H, J = 8.6 Hz, 3H,5H-Ph-Cl), 7.14 – 7.08 (m, 2H, 4H,6H-Ph-OCH₃), 7.01 – 6.95 (m, 1H, 5H-Ph-OCH₃), 3.86 (s, 3H, -OCH₃), 2.34 (s, 3H, 5-CH₃-Thiazol); ¹³C-NMR (63 MHz, DMSO-d⁶, δ): 179.2, 163.1, 153.7, 150.5, 142.6, 132.8, 130.1, 128.5, 120.8, 120.5, 117.0, 112.4, 111.8, 55.7, 11.6; ESI-MS (m/z): 333.8 [M+H⁺]; CHN Calculated: C 49.59%, H 3.92%, N 6.80%, S 7.79%; Found: C 49.32%, H 3.80%, N 6.71%, S 7.84%; Yield: 66 %; Light yellow solid.

3-(4-(4-Chlorophenyl)-5-methylthiazol-2-ylamino)benzoic acid (Compound **9**; Table 2)

¹H-NMR (250 MHz, DMSO-d⁶, δ): 12.89 (s, 1H, -OH), 10.28 (s, 1H, -NH-), 8.25 (s, 1H, 2H-Ph-COOH), 7.94 (d, 1H, J = 7.8 Hz, 6H-Ph-COOH), 7.72 (d, 2H, J = 8.6 Hz, 2H,6H-Ph-Cl), 7.52 – 7.39 (m, 4H, 3H,5H-Ph-Cl, 4H,5H-Ph-COOH), 2.44 (s, 3H, -CH₃); ¹³C-NMR (63 MHz, DMSO-d⁶, δ): 167.3, 158.9, 143.8, 141.2, 133.8, 131.5, 129.5, 129.0, 128.2, 121.6, 120.5, 117.5, 117.3, 11.8; ESI-MS (m/z): 322.2 [M+H⁺]; CHN Calculated: C 52.25%, H 3.76%, N 13.06%, S 19.93%; Found: C 52.30%, H 3.87%, N 13.06%, S 20.24%; Yield: 44 %; Light red solid.

4-(4-(4-Chlorophenyl)-5-methylthiazol-2-ylamino)benzoic acid (Compound **10**; Table 2)

$^1\text{H-NMR}$ (250 MHz, DMSO-d^6 , δ): 10.59 (s, 1H, -NH-), 7.88 (d, 2H, $J = 8.8$ Hz, 2H,6H-Ph-Cl), 7.75 – 7.68 (m, 4H, 3H,5H-Ph-COOH, 2H,6H-Ph-COOH), 7.50 (d, 2H, $J = 8.6$ Hz, 3H,5H-Ph-Cl), 2.43 (s, 3H, -CH₃); $^{13}\text{C-NMR}$ (63 MHz, DMSO-d^6 , δ): 166.9, 158.5, 144.8, 143.8, 133.6, 131.7, 130.6, 129.6, 128.3, 122.6, 118.4, 115.8, 11.9; ESI-MS (m/z): 347,1 [M-H^+]; CHN Calculated: C 47.96%, H 3.31%, N 6.58%, S 7.53%; Found: C 48.21%, H 3.35%, N 6.65%, S 7.60%; Yield: 29 %; Yellow powder.

4-(4-(4-Chlorophenyl)-5-methylthiazol-2-yloxy)phenole (Compound **11**; Table 2)

$^1\text{H-NMR}$ (400 MHz, DMSO-d^6 , δ): 9.64 (s, 1H, -OH), 7.60 (d, 2H, $J = 8.6$ Hz, Ph-Cl-2H,6H), 7.48 (d, 2H, $J = 8.5$ Hz, Ph-Cl-3H,5H), 7.18 (d, 2H, $J = 8.9$ Hz, Ph-OH-3H,5H), 6.82 (d, 2H, $J = 8.8$ Hz, Ph-OH-2H,6H), 2.41 (s, 3H, -CH₃); $^{13}\text{C-NMR}$ (75 MHz, DMSO-d^6 , δ): 169.86, 155.55, 147.33, 142.81, 133.11, 131.95, 129.62, 128.33, 122.14, 121.58, 116.17, 12.31; ESI-MS (m/z): 318.8 [M+H^+]; CHN Calculated: C 60.47%, H 3.81%, N 4.41%, S 10.09%; Found: C 60.47%, H 3.47%, N 4.35%, S 10.06%; Yield: 29 %; Light brown solid.

2-(*N*-(4-(4-Chlorophenyl)-5-methylthiazol-2-yl)acetamido)phenyl acetate (Compound **12**; Table 2)

$^1\text{H-NMR}$ (250 MHz, DMSO-d^6 , δ): 7.67 (d, 1H, $J = 7.7$ Hz, Ph-OH-6H), 7.58 (t, 1H, $J = 7.7$ Hz, Ph-OH-5H), 7.46 (d, 1H, $J = 7.6$ Hz, Ph-OH-3H), 7.43-7.37 (m, 5H, Ph-Cl, Ph-OH-4H), 2.47 (s, 3H, Thiazol-CH₃), 2.03 (s, 3H, O-C(O)-CH₃), 1.98 (s, 3H, N-C(O)-CH₃); $^{13}\text{C-NMR}$ (63 MHz, DMSO-d^6 , δ): 169.89, 155.21, 152.99, 142.00, 133.64, 131.58, 130.22, 129.29, 128.19, 126.72, 122.86, 119.60, 116.71, 22.56, 11.55; ESI-MS (m/z): 401.1 [M+H^+]; CHN Calculated: C 59.92%, H 4.27%, N 6.99%, S 8.00%; Found: C 59.82%, H 4.20%, N 6.98%, S 7.92%; Yield: 46 %; Yellow needles.

2-(*N*-(5-Acetyl-4-(4-chlorophenyl)thiazol-2-yl)acetamido)phenyl acetate (Compound **13**; Table 2)

$^1\text{H-NMR}$ (250 MHz, DMSO-d^6 , δ): 7.71 (d, 1H, $J = 7.71$ Hz, Ph-OH-3H), 7.57 (t, 1H, $J = 7.77$ Hz, Ph-OH-5H), 7.47-7.39 (m, 6H, Ph-OH-4H,6H, Ph-Cl), 2.20 (s, 3H, Thiazol-C(O)-CH₃), 2.06 (s, 3H, O-C(O)-CH₃), 2.04 (s, 3H, N-C(O)-CH₃); $^{13}\text{C-NMR}$ (63 MHz, DMSO-d^6 , δ): 191.19, 170.60, 168.17, 159.52, 151.78, 146.42, 133.88, 133.28, 131.21, 131.00, 130.67, 130.65, 128.41, 127.99, 127.00, 124.04, 29.64, 22.92, 20.19; ESI-MS (m/z): 429.8 [M+H^+]; CHN Calculated: C 58.81%, H 4.00%, N 6.53%, S 7.48%; Found: C 59.10%, H 4.08%, N 6.49%, S 7.53%; Yield: 57 %; White solid.

4-(4-Chlorophenyl)-2-(4-hydroxyphenylamino)thiazole-5-carboxamide (Compound **19**; Table 2)

$^1\text{H-NMR}$ (250 MHz, DMSO-d^6 , δ): 10.14 (s, 1H, -NH-), 9.22 (s, 1H, -OH), 7.70 (d, 2H, $J = 8.5$ Hz, Ph-Cl-2H,6H), 7.47 (d, 2H, $J = 8.5$ Hz, Ph-Cl-3H,5H), 7.37 (d, 2H, $J = 8.8$ Hz, Ph-OH-3H,5H), 7.22 (br, 2H, -NH₂),

6.74 (d, 2H, J = 8.8 Hz, Ph-OH-2H,6H); ¹³C-NMR (63 MHz, DMSO-d⁶, δ): 163.43, 162.78, 153.01, 149.92, 133.45, 132.78, 132.26, 130.65, 127.87, 120.17, 115.45, 115.01; ESI-MS (m/z) 346.8 [M+H⁺]; CHN Calculated: C 55.57%, H 3.50%, N 12.15%, S 9.27%; Found: C 55.31%, H 3.50%, N 11.76%, S 9.63%; Yield: 69 %; White solid.

2.2. Evaluation of DNase I and 5-LO inhibition

4-(4-Chlorophenyl)thiazol-2-amines **1-20** were investigated for the inhibitory effect towards bovine pancreatic DNase I. The *in vitro* evaluation of DNase I inhibition is based on spectrophotometric measurement of acid-soluble nucleotides formation at 260 nm according to the method previously described [28–33], using crystal violet as a positive control.

Inhibition of 5-LO activity was determined both in an intact cell system using freshly isolated polymorphonuclear leukocytes (PMNL) and in a cell-free assay using partially purified recombinant 5-LO and 5-LO product formation was determined by HPLC according to the method previously described [36].

2.3. *In silico* studies

2.3.1. Pharma/E-State RQSAR models

Pharma/E-State RQSAR models analyzed the 4-(4-chlorophenyl)thiazol-2-amines activity as a function of the type of R-group at each attachment position, and displayed the results qualitatively in terms of increasing, decreasing, or little effect on the activity [37]. We ran a partial-least-squares (PLS) procedure that fitted the observed inhibitory data to the counts of the features present in each R-group at each position. For Pharma/E-State RQSAR models, the features counted are the pharmacophore types and various E-state atom types [37]. This was done using a 75% : 25% random training : test-set split. The procedure was repeated 100 times, picking each time the model that does the best job without overfitting. For each model, each pharmacophore/E-state feature type at each R-group position was given a coefficient that reflects how much it contributes to the property being modeled. A feature type was deemed significant (colored red or blue) if the absolute value of the mean of its coefficients over the models exceeded the importance cutoff, which is a statistic computed from all coefficients over all models.

2.3.2. Molecular docking

2.3.2.1. Ligand preparation

Selected 4-(4-chlorophenyl)thiazol-2-amines were generated using the builder panel in Maestro [37] and subsequently optimized using the LigPrep [37]. Partial atomic charges were ascribed and possible

ionization states were generated at a pH of 7.0. The OPLS-2005 force field was used for optimization and the resulting structures were used for modeling studies.

2.3.2.2. Receptor preparation

The X-ray crystallographic structures of DNase I (PDB code: 1DNK) and 5-LO (PDB code: 3O8Y), retrieved from the Protein Data Bank, were prepared using the Protein Preparation Wizard [37]. Following the assignment of charge and protonation state, energy minimization till RMSD value of 0.30 Å was done using the OPLS-2005 force field. The SiteMap [37] was used to identify possible ligand-binding pockets within the optimized structure of DNase I and 5-LO. Using Glide [37], a grid box with a 10 Å radius was generated at the centroid of the top-ranked binding pocket obtained by SiteMap [37].

2.3.2.3. Docking protocol

Selected 4-(4-chlorophenyl)thiazol-2-amines were docked into the top-ranked binding pocket of DNase I and 5-LO using Glide [37]. The standard precision mode without applying any constraints was used for the flexible docking. Each enzyme/inhibitor complex with lowest Glide docking score was selected for further study.

2.3.3. Molecular dynamics simulation

The molecular dynamics simulation of the most active 4-(4-chlorophenyl)thiazol-2-amines was carried out using Desmond [37]. Forcefield parameters for the enzyme/inhibitor system were assigned using the OPLS-2005 force field. The structure of the added water was based on the simple point charge (SPC) solvent model. The system was neutralized with Na⁺ ions to balance the net charge of the whole simulation box to neutral. The final system contained approximately 26100 atoms for DNase I and 136900 atoms for 5-LO. The system was passed through a 6-step relaxation protocol before molecular dynamics simulations. The relaxed system was simulated for 10 ns, using a normal pressure temperature (NPT) ensemble with a Nosé–Hoover thermostat at 300 K and Martyna–Tobias–Klein barostat at 1.01325 bar pressure. Atomic coordinate data and system energies were recorded every 1 ps. The root mean square deviation (RMSD) and root mean square fluctuation (RMSF) of the enzyme/inhibitor complexes were analyzed with respect to the simulation time.

2.3.4. Pharmacophore modeling and virtual screening

Pharmacophore mapping was carried out using PHASE version 4.2 available in Maestro 10.1 molecular modeling package from Schrödinger [38]. Pharmacophore modeling is the qualitative picture for

Journal Pre-proofs

finding the chemical feature for the active site geometry and spatial arrangements in 3D space of the ligands. There are 6 in-built pharmacophore features available in PHASE: hydrogen bond acceptor (A), hydrogen bond donor (D), hydrophobic group (H), negative charged group (N), positive charged group (P) and aromatic ring (R). Common pharmacophore features were used to construct pharmacophore sites. For defining the most active pharm - set in PHASE, an activity threshold range was selected in such a way that compounds were active if IC_{50} value was below 100 μ M and inactive if IC_{50} value was above 100 μ M. The common pharmacophore hypotheses were generated with default settings. A pharmacophore cluster was proceeded based on the highest average similarity. The preferred hypothesis was then selected based on the survival score. The PubChem database consisting of more than 96 million compounds was subjected to pharmacophore based virtual screening using the top ranked hypothesis. The advanced pharmacophore screening option from PHASE module was employed to retrieve hit compounds that fulfill the chemical moiety necessities and spatially mapping with subsequent features in the pharmacophoric query [38].

2.3.5. *In silico* study of the physico-chemical, pharmacokinetic and toxicological properties

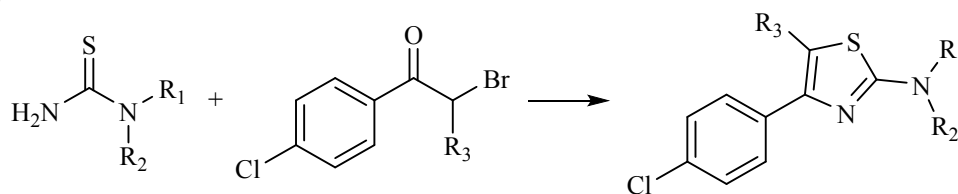
In silico study of the physico-chemical, pharmacokinetic and toxicological properties of the most potent DNase I inhibitors was performed using Molinspiration [39], admetSAR [40], and DataWarrior [41] prediction tools.

3. RESULTS AND DISCUSSION

3.1. Synthesis and DNase I inhibitory properties of 4-(4-chlorophenyl)thiazol-2-amines

3.1.1. Synthesis

Eleven new 4-(4-chlorophenyl)thiazol-2-amines (**3-6**, **8-13**, **19**) were synthesized by Hantzsch-thiazole synthesis illustrated in Scheme 1 [35]. Together with nine previously synthesized derivatives (**1** [34], **2**, **7** [35], **14** [36] **15-17** [35], **18** [36], **20** [36]), they were evaluated *in vitro* for the inhibitory activity against bovine pancreatic DNase I. The obtained results were plotted and IC_{50} values were calculated (Table 2).

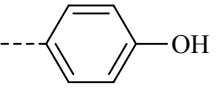
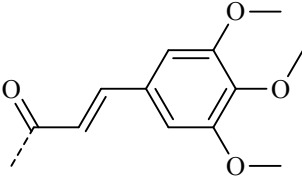
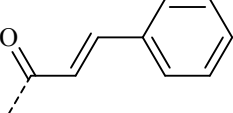
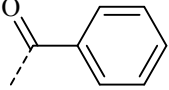


Scheme 1. Synthesis of 4-(4-chlorophenyl)thiazol-2-amines.

Starting from the scaffold of compound **1**, SAR analysis of the substituted 4-(4-chlorophenyl)thiazol-2-amines was performed focusing on the optimization. It was observed that variation of R2 substituents (including heteroaromatic substituents) showed no differences in DNase I inhibition (compounds **1-8**). Introduction of the bulkier methyl group in R3 position accompanied with phenylcarboxylic acids (**9** and **10**) or phenylcarboxylic esters (**11** and **12**) as R2 substituents showed decreased IC₅₀ values (below 150 μM). An introduction of an electron-pulling substituent (acetyl) in R3 position of compound **12** resulted in some improvement of the IC₅₀ value (106.63 μM for compound **13**). In the next step, the influence of different R2 aromatic substituents on DNase I inhibition was examined (compounds **14-17**), where compound **17** showed the most promising inhibitory properties. Therefore, this *para*-hydroxy-phenyl substituent was further incorporated in compounds **18-20** which also contained electron-pulling groups in R3 position (previously shown beneficial in compound **13**). As a result, IC₅₀ values below 100 μM were reached (Table 2). Crystal violet, used as a positive control in the absence of a "golden standard", showed almost 5-fold weaker inhibitory effect on commercial DNase I (IC₅₀ = 359.05 ± 7.18 μM) compared to the three most active compounds **18-20**.

Table 2

In vitro DNase I inhibitory activity of the studied 4-(4-chlorophenyl)thiazol-2-amines.

Compd.	R1	R2	R3	DNase I inhibition IC ₅₀ (μM) ± SD
1 [34-36]	-H		-H	>200
2 [35]	-H		-H	>200
3	-H		-H	>200
4	-H		-H	>200

6	-H		-CH ₃	>200
7 [35]	-H		-CH ₃	>200
8	-H		-CH ₃	>200
9	-H		-CH ₃	136.84 ± 11.11
10	-H		-CH ₃	142.01 ± 14.87
11	-H		-CH ₃	105.21 ± 14.32
12			-CH ₃	126.02 ± 10.53
13				106.63 ± 15.70
14 [36]	-H		-CH ₃	>200
15 [35]	-H		-CH ₃	>200
16 [35]	-H		-CH ₃	172.12 ± 10.61
17 [35,36]	-H		-CH ₃	130.75 ± 11.83
18 [36]	-H			81.30 ± 8.12
19	-H			79.79 ± 7.04

3.1.3. R-Group analysis

As Pharma RQSAR model showed, the substantial increase in DNase I inhibition was a consequence of hydrogen-bond acceptor substituents at 4-(4-chlorophenyl)thiazol-2-amine scaffold (Table S1, Fig. 1). Furthermore, negatively-charged substituents at R1 position, along with hydrogen-bond donor and hydrophobic substituents at R3 position, exerted significant enhancement to the 4-(4-chlorophenyl)thiazol-2-amines activity (Table S1, Fig. 1). Additionally, the presence of hydrophobic substituents at R1 position resulted in a decreased DNase I inhibition (Table S1, Fig. 1). Next, we examined the effect of the E-State parameters of 4-(4-chlorophenyl)thiazol-2-amines on DNase I inhibition (Table S2, Fig. 2). As Table S2 shows, the introduction of aasC, dssC, aaCH, ssO, sOH and dO fragments at R1 position, dssC and dO fragments at R2 position, as well as the introduction of aasC, dssC, tsC, sNH₂, tN and dO fragments at R3 position, exerted a significant enhancement to the 4-(4-chlorophenyl)thiazol-2-amines activity. On the contrary, the use of ssS, sCH₃ and aaN fragments at R1 position, as well as the introduction of aaCH fragment at R3 position, resulted in a decreased DNase I inhibition (Table S2, Fig. 2).

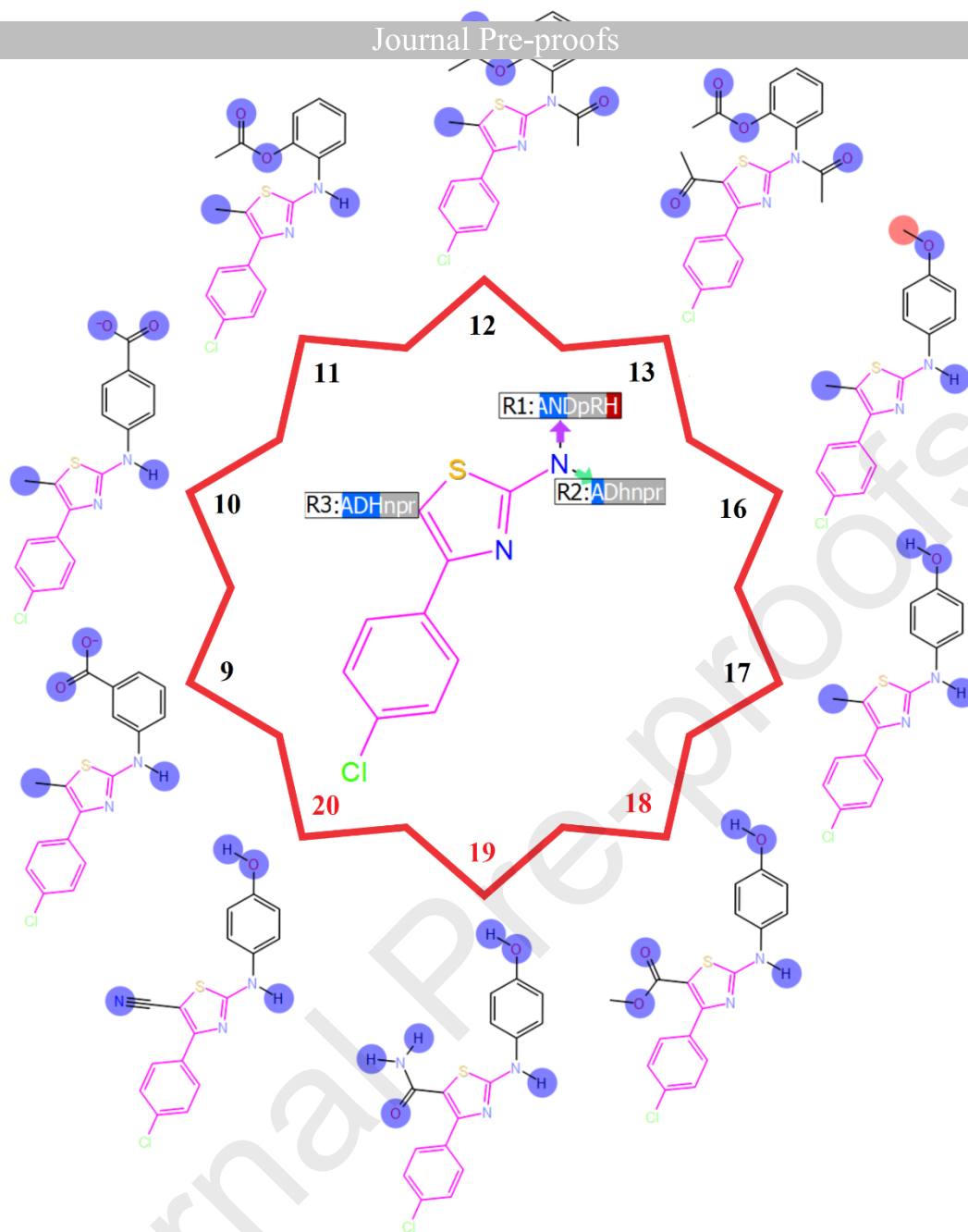


Fig. 1. The Pharma RQSAR model of the investigated series of 4-(4-chlorophenyl)thiazol-2-amines. The attachment positions on the 4-(4-chlorophenyl)thiazol-2-amine scaffold were labeled with a list of pharmacophore features, colored by significance: blue for significant positive contributions, red for significant negative contributions, and gray for insignificant contributions to DNase I inhibition. If a pharmacophore feature was absent from an attachment position, a lower-case letter was used for the pharmacophore feature type. Examined pharmacophore features: hydrogen-bond acceptor (A), hydrogen-bond donor (D), hydrophobic (H), negatively-charged (N), positively-charged (P), and aromatic (R).

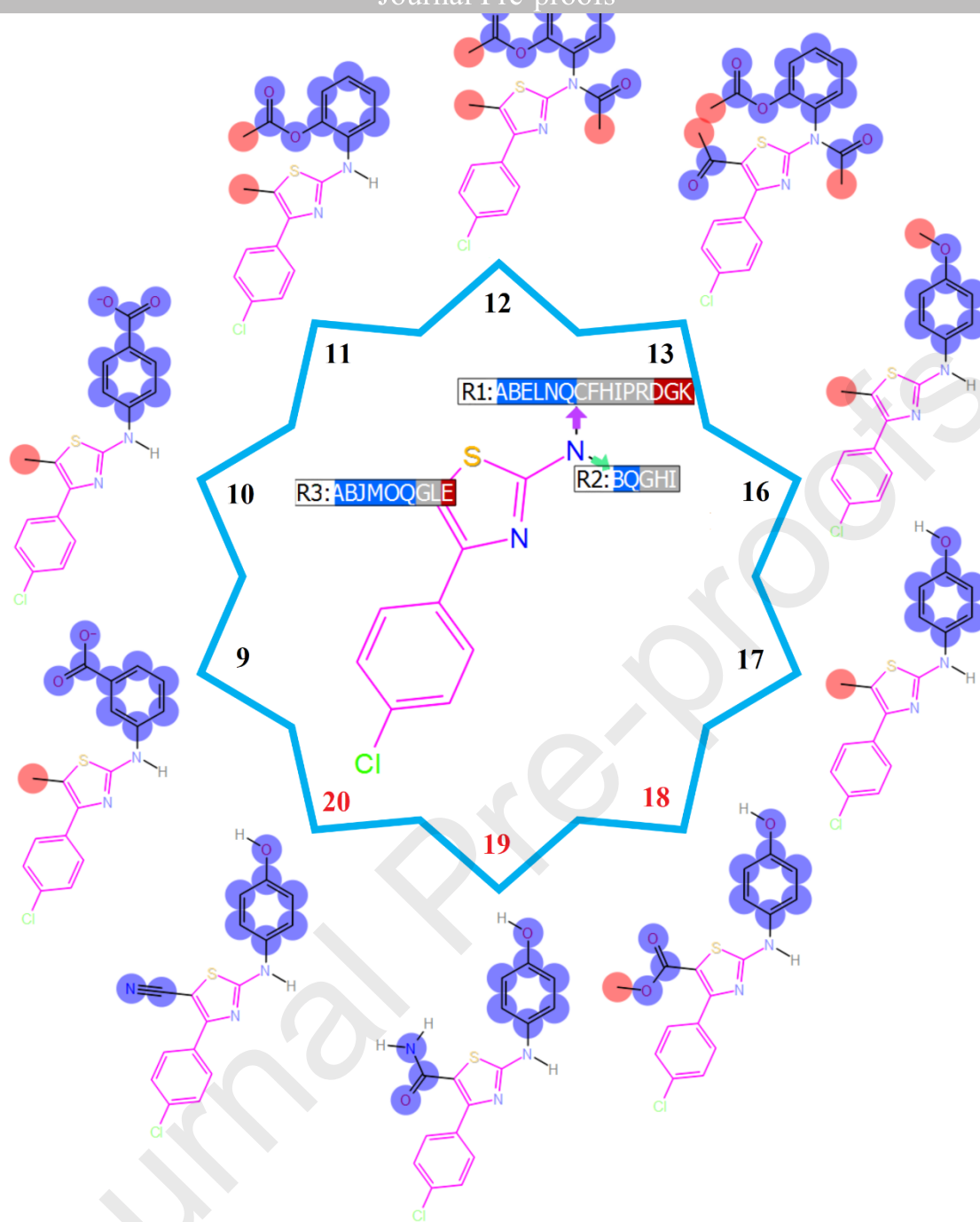


Fig. 2. The E-State RQSAR model of the investigated series of 4-(4-chlorophenyl)thiazol-2-amines. The attachment positions on the 4-(4-chlorophenyl)thiazol-2-amine scaffold were labeled with a list of letters representing the E-state atom types (Table S2), colored by significance: blue for significant positive contributions, red for significant negative contributions, and gray for insignificant contributions to DNase I inhibition. If an E-state atom type was absent from an attachment position, it was not included in the annotation for that position.

3.1.4.1. Molecular docking

Our recent *in silico* results showed that amino acid residues like Asn 7, Arg 9, Glu 39, Arg 111, His 134, Pro 137, Asp 168, Asn 170, Thr 203, Thr 205, Thr 207, Tyr 211, Asp 251 and His 252 constituted the binding pocket of the DNase I structure [28]. It is worth mentioning that inhibitor-binding pocket, represented by a boxed surface map, is within the region that interacts with DNA octamer d(GGTATACC)₂ (Fig. 3A). Of note, the importance of His 134 and His 252 residues in the catalytic mechanism of DNase I has already been highlighted [42]. It was confirmed that catalytic residues His 134 and His 252 are a part of the ion binding site IV, which is implicated in the cleavage of scissile phosphate [43]. Furthermore, several site-directed mutagenesis experiments on the residues surrounding His 134 and His 252 demonstrated that single mutations on Glu 39, Asp 168 or Asp 251 residues lead to the inactive DNase I variants [44]. Additionally, the critical role of Arg 9, Arg 41, Tyr 76, Arg 111, Asn 170, Tyr 175 and Tyr 211 residues in DNase I activity was confirmed, presumably because of their close proximity to the active site [44].

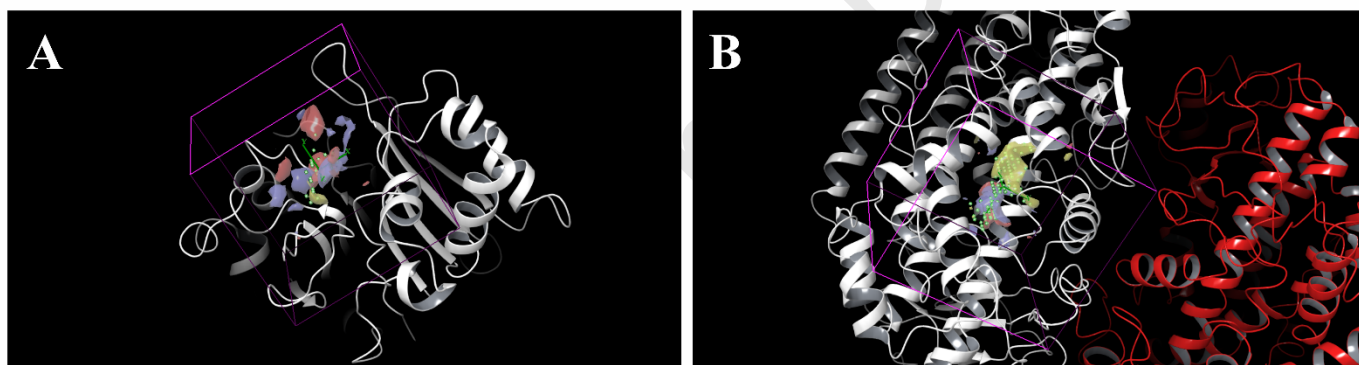


Fig. 3. The top ranked DNase I (A) and 5-LO enzyme (B) binding site, represented by the boxed surface maps.

The intermolecular contacts between most active 4-(4-chlorophenyl)thiazol-2-amines and DNase I were analyzed using the ligand interaction diagram in Maestro [37]. The interaction profiles of 4-(4-chlorophenyl)thiazol-2-amines with DNase I domain are displayed in Fig. 4. Showing interactions with catalytic histidines (His 134 or His 252), compounds **18-20** were the most promising inhibitors of DNase I (Table 2, Fig. 4). Additionally, these compounds exhibited some interactions with Arg 9, Glu 39, Arg 41, Tyr 76, Arg 111, Asp 168, Asn 170, Tyr 175, Tyr 211 and Asp 251 (Fig. 4), which are also implicated in a DNase I activity [42–44]. Furthermore, compound **19** as the most active DNase I inhibitor (Table 2), uniquely showed interactions with both catalytic histidines (Fig. 4).

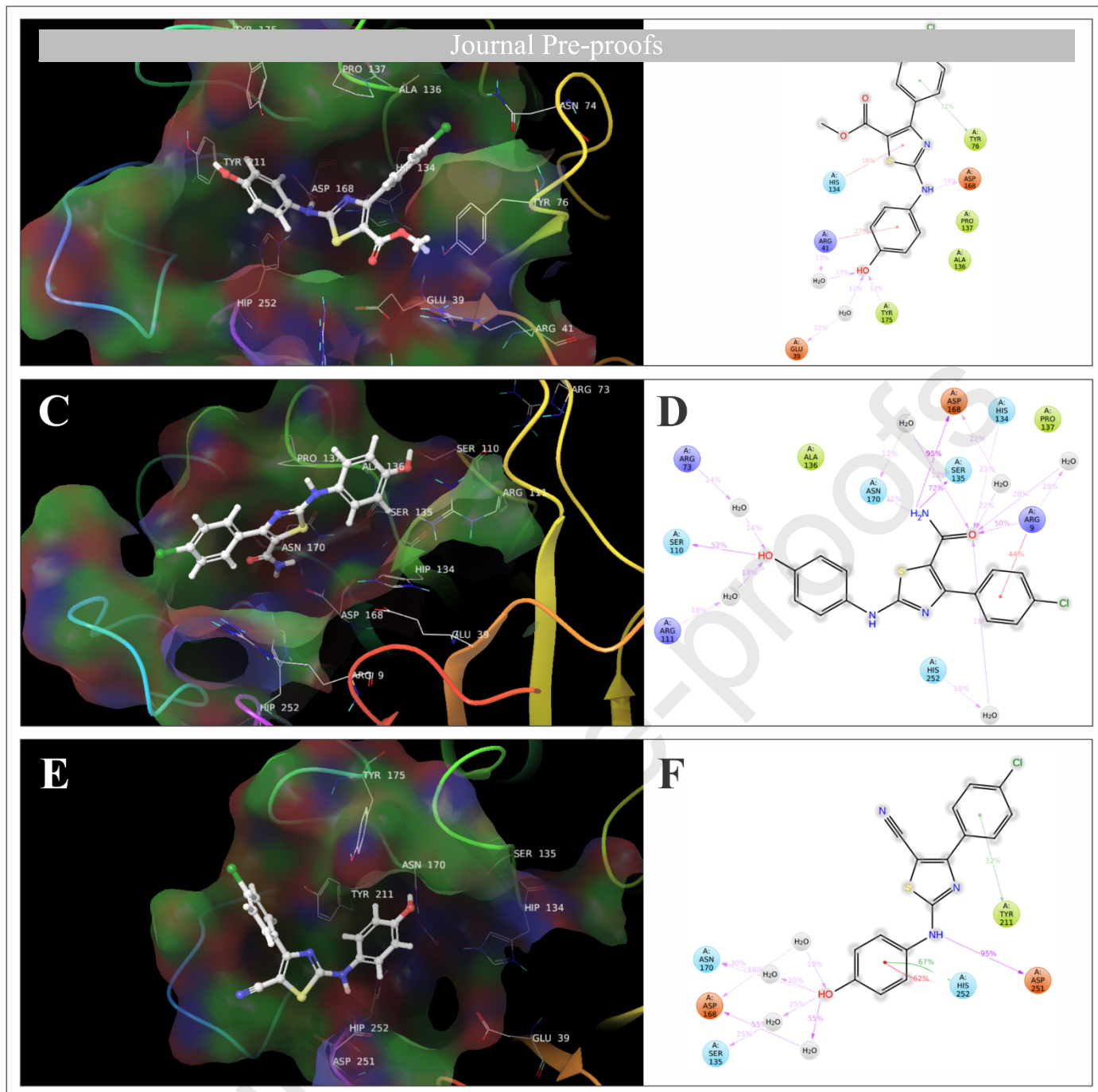


Fig. 4. 3D/2D view of compounds **18** (A,B), **19** (C,D) and **20** (E,F) bound in the active site of DNase I. Interactions that occur more than 10% of the molecular dynamics simulation time are shown.

3.1.4.2. Molecular dynamics simulation

The study was further extended to assess the stability of docking complexes between DNase I and the most active 4-(4-chlorophenyl)thiazol-2-amines through molecular dynamics simulations (Animation contents S1-S3). The RMSD and RMSF plots for DNase I and compounds **18-20** (Figs. S1 and S2) showed that docking complexes were stable during entire simulation period. The RMSD for C α , side chains and heavy atoms remained within the limit of 3 Å (Fig. S1). The similar situation was noted for RMSF values (Fig. S2).

The obtained results indicated small structural rearrangements, less conformational changes and confirmed stability of DNase I complexes [37]. Once the conformational stability of the systems was established, the interaction stability of the systems was monitored. The interactions observed during 10 ns molecular simulation confirmed the importance of Arg 9, Glu 39, Arg 41, Tyr 76, Arg 111, His 134, Asp 168, Asn 170, Tyr 175, Tyr 211, Asp 251 and His 252 in the binding with the most active 4-(4-chlorophenyl)thiazol-2-amines (Figs. 4-7, Animation contents S1-S3). The continuity of interactions between DNase I and the inhibitors is clearly expressed by percentage of overall simulation time (Fig. 4). As a consequence of the number, type and continuity of interactions with catalytic histidines (His 134 and His 252), it is distinctly clear why compound **19** is stronger DNase I inhibitor compared to compounds **18** and **20** (Figs. 4-7).

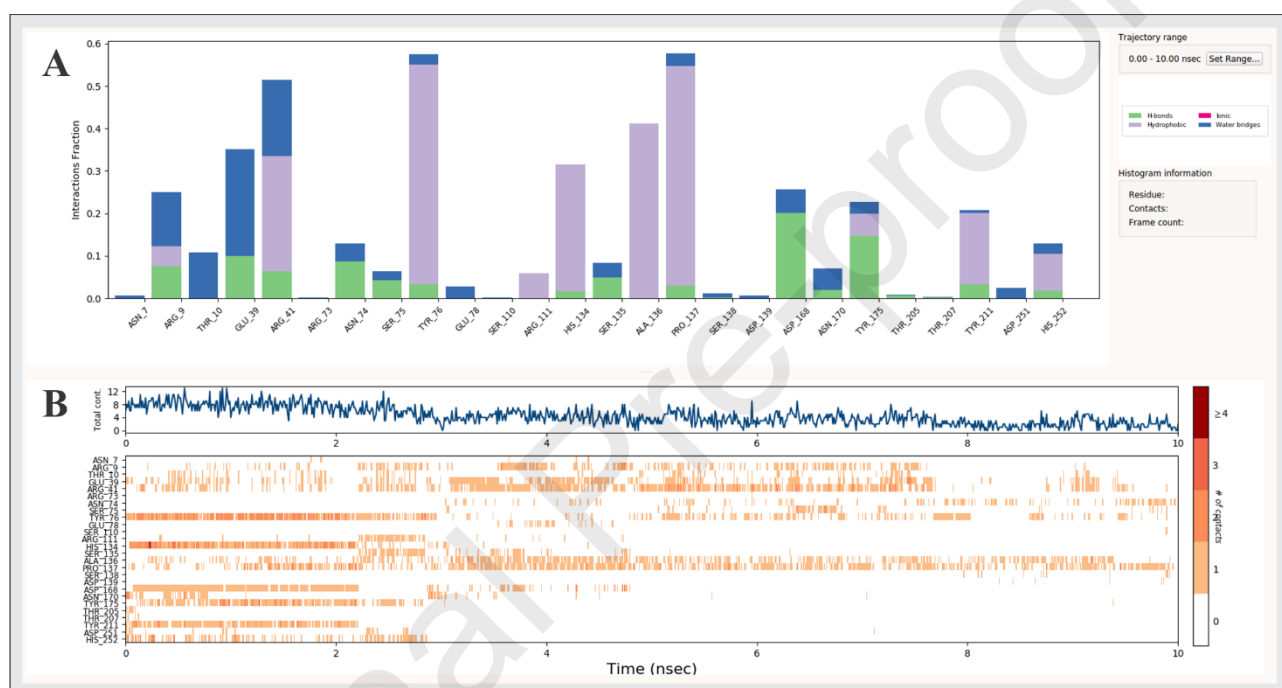


Fig. 5. Normalized stacked bar chart representation and timeline representation of interactions and contacts between bovine pancreatic DNase I and compound **18** during the course of 10 ns molecular dynamics simulation.

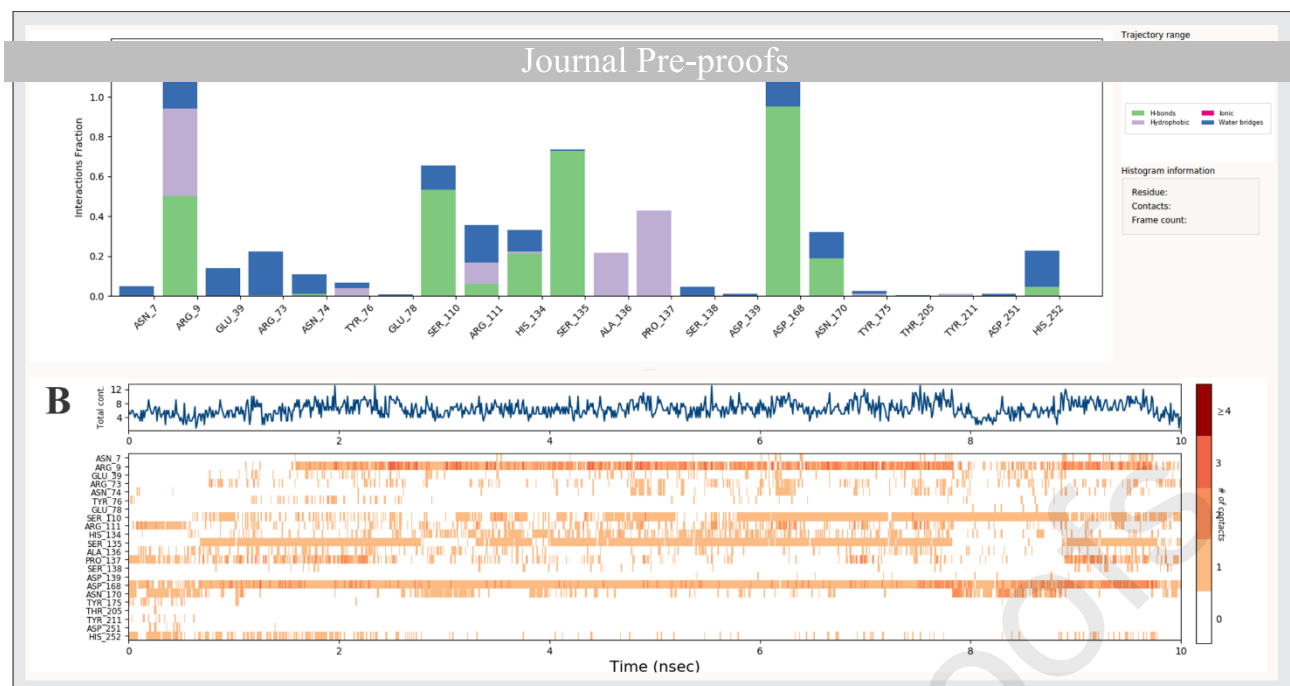


Fig. 6. Normalized stacked bar chart representation and timeline representation of interactions and contacts between bovine pancreatic DNase I and compound **19** during the course of 10 ns molecular dynamics simulation.

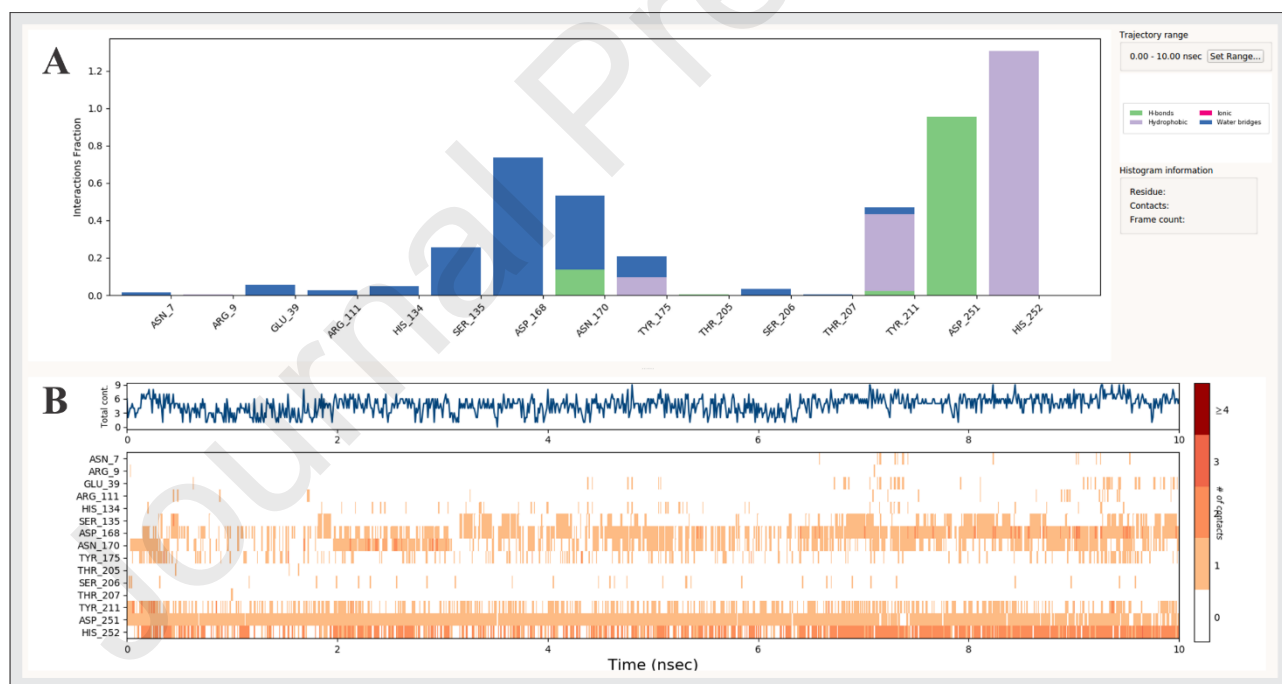


Fig. 7. Normalized stacked bar chart representation and timeline representation of interactions and contacts between bovine pancreatic DNase I and compound **20** during the course of 10 ns molecular dynamics simulation.

3.1.5. Pharmacophore modeling and virtual screening

The best hypothesis model for the studied 4-(4-chlorophenyl)thiazol-2-amines was selected by analyzing the survival scores in Table S3. The selected AADHRRR.13 hypothesis had 7 features namely, 2 acceptor groups (A), 1 donor group (D), 1 hydrophobic group (H) and 3 aromatic groups (R). The structural superposition of most active 4-(4-chlorophenyl)thiazol-2-amines with AADHRRR.13 hypothesis is presented in Fig. 8. The angle and distances between different sites of the model are given in Tables S4 and S5, respectively. The AADHRRR.13 hypothesis highlighted the 3D space arrangement among hydrogen-bond substituents and aromatic rings at 4-(4-chlorophenyl)thiazol-2-amines (Fig. 8) and confirmed the importance of selected groups in DNase I inhibition (Fig. 4). The PubChem database consisting of more than 96 million compounds was subjected to virtual screening using the 4-(4-chlorophenyl)thiazol-2-amine scaffold. Ligand-based virtual screening, retrieved 119 hit compounds that fulfilled the chemical moiety necessities of 4-(4-chlorophenyl)thiazol-2-amines (Table S6). In order to find a virtual candidate for DNase I inhibition, pharmacophore AADHRRR.13 hypothesis was applied on selected molecules. The results showed that none of the selected molecules fulfilled the 3D space requirements of AADHRRR.13 hypothesis. These observations could be potentially utilized to guide the rational design of novel/potent DNase I inhibitors with 4-(4-chlorophenyl)thiazol-2-amine moiety.

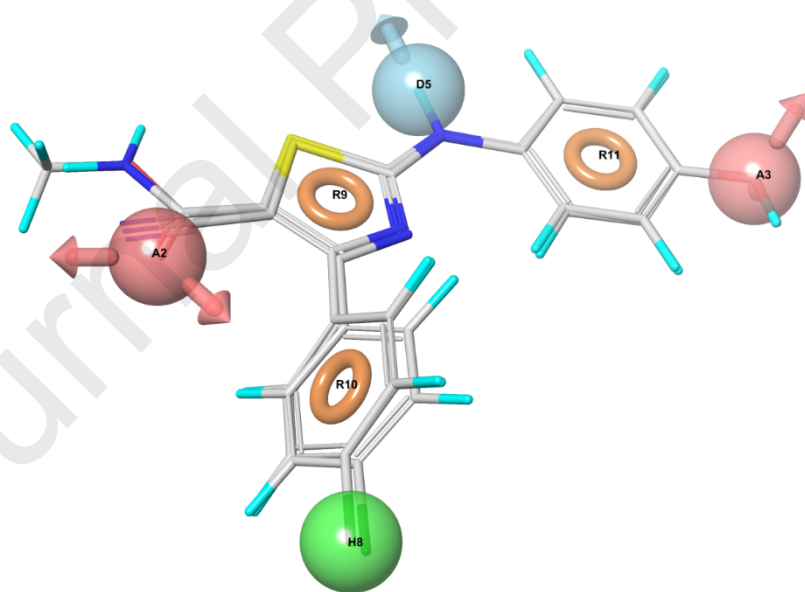


Fig. 8. Superimposed structures of the three most active 4-(4-chlorophenyl)thiazol-2-amines with AADHRRR.13 hypothesis.

3.2. 5-LO inhibition

Compounds **18** and **20** were previously reported as potent 5-LO inhibitors [36]. In order to obtain complete picture of 5-LO inhibitory properties of the three most potent DNase I inhibitors within the investigated series (**18-20**), compound **19** was also evaluated on 5-LO inhibition. Results are shown in Table 3.

Table 3

5-LO inhibitory activity of compounds **18-20**.

Compd.	WT 5-LO inhibition [IC ₅₀] (95% CI, n ≥ 3)	PMNL 5-LO inhibition [IC ₅₀] (95% CI, n ≥ 3)	Reference on 5-LO inhibition
18	0.08 (0.063 – 0.110)	0.62 (0.46 – 0.83)	[36]
19	0.63 (0.39 – 1.02)	36.47 ± 5.36 Residual activity at 10 μM ± SEM[%]#	/
20	0.05 (0.03 – 0.07)	1.11 (0.93 – 1.32)	[36]

Measured in cell-free assay (WT) and intact (PMNL) given as IC₅₀ (μM) with 95% confidence intervals (CI)

#Residual activity at 10 μM ± standard error of the mean (%)

PMNL: Polymorphonuclear leukocytes; SEM: Standard error of the mean; WT: Wild-type

This (5-LO) enzyme, able to oxidize fatty acids and thereby synthesize leukotrienes, potent mediators of oxidative and inflammatory reactions, is expressed in the central nervous system (CNS) neurons and may participate in neurodegeneration [45–48]. It was shown that the levels of 5-LO and its metabolites (leukotrienes) are increased in elderly subjects contributing to the development of neurodegenerative disorders, including Alzheimer's disease, as one of the most common and most studied aging-associated neurodegenerative disorders [45,49–52]. Thus, the inhibition of 5-LO presents a promising target for neuroprotective therapies [45,50,52]. As aging is associated with enhanced DNA fragmentation and activation of apoptotic machinery [53], DNase I also represents an attractive potential target do design alternative strategies for the treatment of neurodegenerative disorders (Alzheimer's disease).

3.2.1.1. Molecular docking

By combining a novel and highly effective algorithm for rapid binding-site evaluation with easy-to-use property visualization tools, SiteMap provides researchers with an efficient means to identify and characterize binding sites [54]. The results from the SiteMap analysis highlighted that amino acid residues like Phe 177, Tyr 181, His 367, Leu 368, His 372, Leu 414, Phe 421, Trp 599, His 600, Ala 603 and Leu 607 constituted the top-ranked binding pocket of 5-LO enzyme (Table S7, Fig. 3B). Of note, the importance of His 367 and His 372 residues in the catalytic site of 5-LO enzyme has already been highlighted [55,56]. It is worth mentioning that Leu 368, Leu 414 and Leu 607 form a constellation of branched hydrophobic side chains that envelops the region where the fatty acid must be positioned for catalysis [56]. Furthermore, it was shown that Phe 177, Tyr 181, Phe 421, Trp 599, His 600 and Ala 603 cork the catalytic site of 5-LO enzyme [56].

The interaction profiles of 4-(4-chlorophenyl)thiazol-2-amines with 5-LO domain are displayed in Fig. 9. Showing interactions with His 372 residue in the catalytic site of 5-LO enzyme, compounds **18-20** exhibited potent activities with inhibitory concentration values in the nanomolar concentration range (Table 3, Fig. 9). Additionally, these compounds exhibited some interactions with Phe 177, Tyr 181, Phe 421, Trp 599 and His 600 (Fig. 9), which are also implicated in a 5-LO activity [55,56].

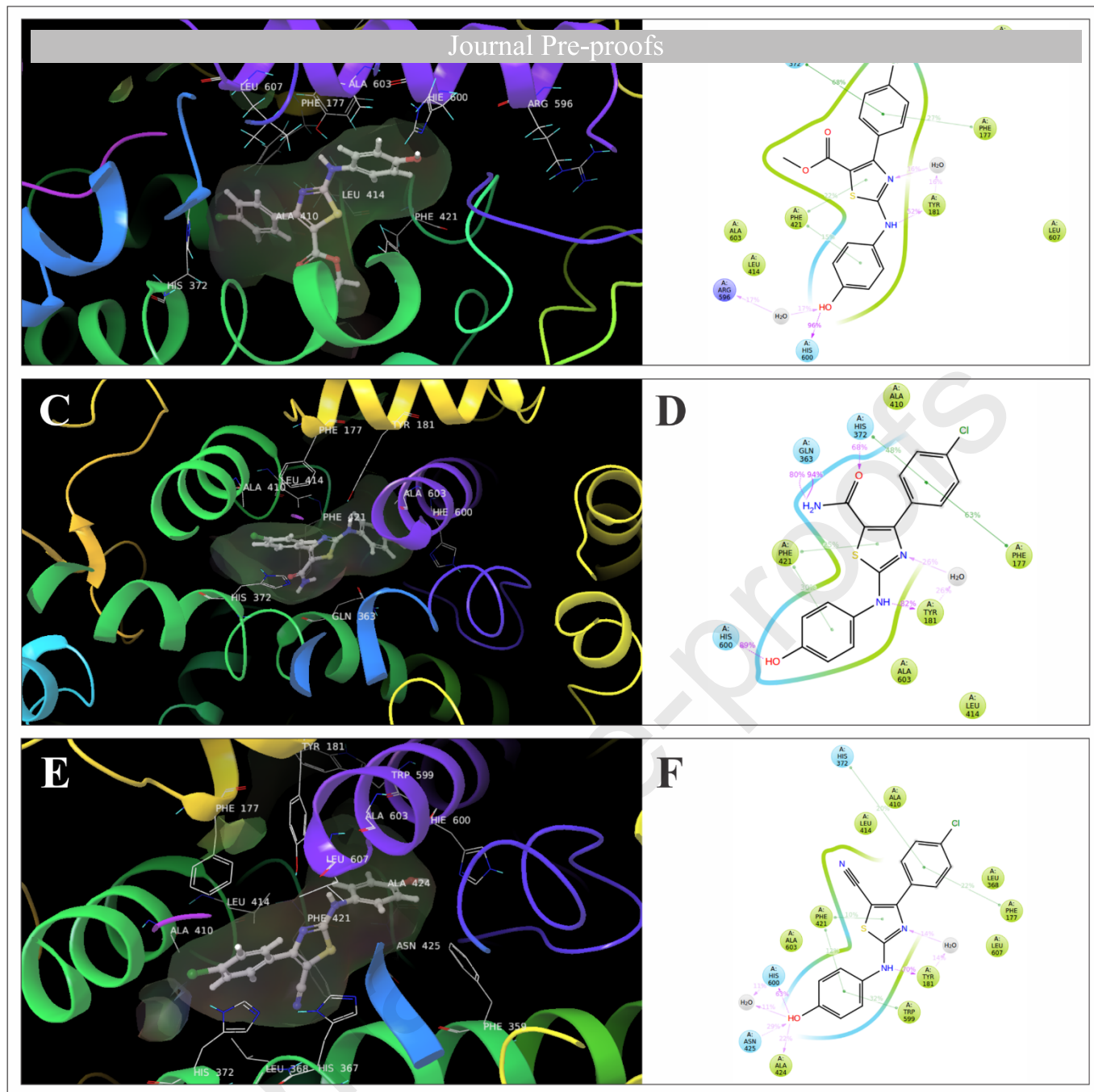


Fig. 9. 3D/2D view of compounds **18** (A,B), **19** (C,D) and **20** (E,F) bound in the active site of 5-LO enzyme. Interactions that occur more than 10% of the molecular dynamics simulation time are shown.

3.2.1.2. Molecular dynamics simulation

The study was further extended to assess the stability of docking complexes between 5-LO and compounds **18-20** through the molecular dynamics simulations (Animation contents S4-S6). The RMSD and RMSF plots for 5-LO and compounds **18-20** (Figs. S3 and S4) also confirmed that docking complexes were stable during entire simulation period. The interactions observed during 10 ns molecular simulation confirmed the importance of Phe 177, Tyr 181, His 367, Leu 368, His 372, Leu 414, Phe 421, Trp 599, His 600, Ala 603

and Leu 607 in the binding with compounds **18-20** (Fig. 9, Figs. 10-12. Animation contents S4-S6). The continuity of interactions between 5-LO and the inhibitors are clearly expressed by percentage of overall simulation time (Fig. 9). It is worth mentioning that compounds **18** and **20** as the most active 5-LO inhibitors (Table 3), uniquely showed interactions with both catalytic histidines compared to less active compound **19** (Figs. 10-12). It could be concluded that compounds **18-20**, as dual 5-LO and DNase I inhibitors, could be set as a promising tool for the development of novel therapeutics used in the prevention and/or therapy of Alzheimer's disease.

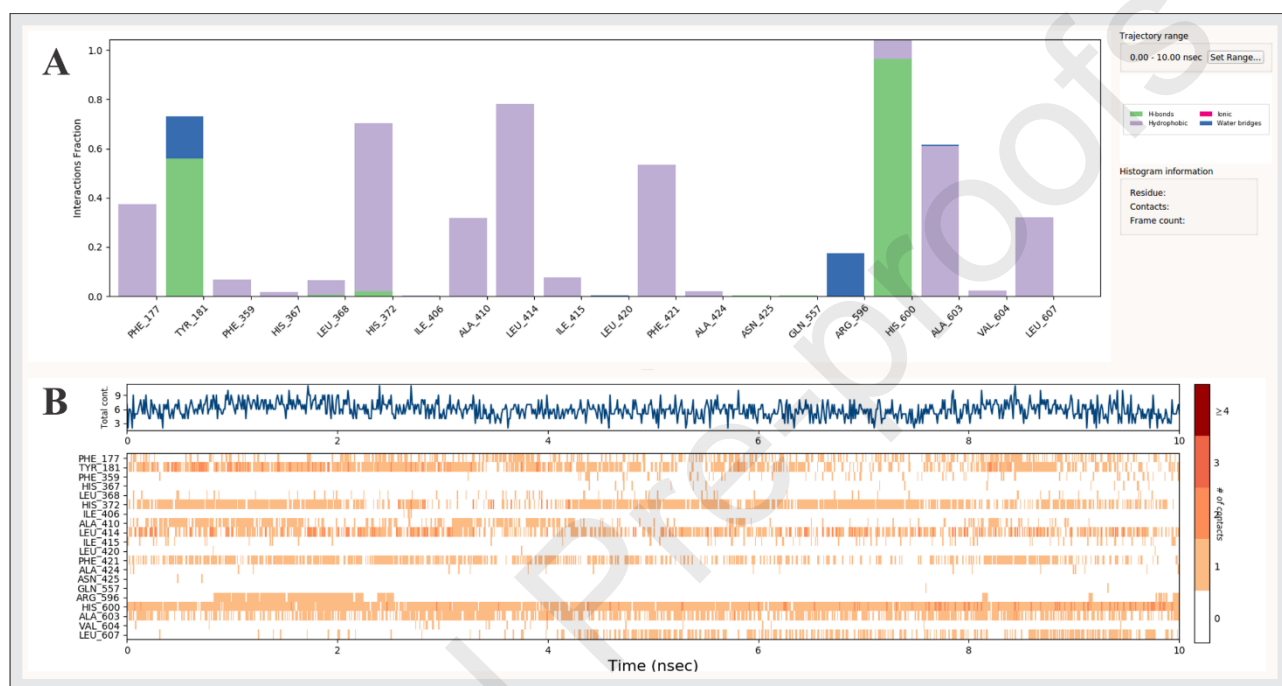


Fig. 10. Normalized stacked bar chart representation and timeline representation of interactions and contacts between 5-LO enzyme and compound **18** during the course of 10 ns molecular dynamics simulation.

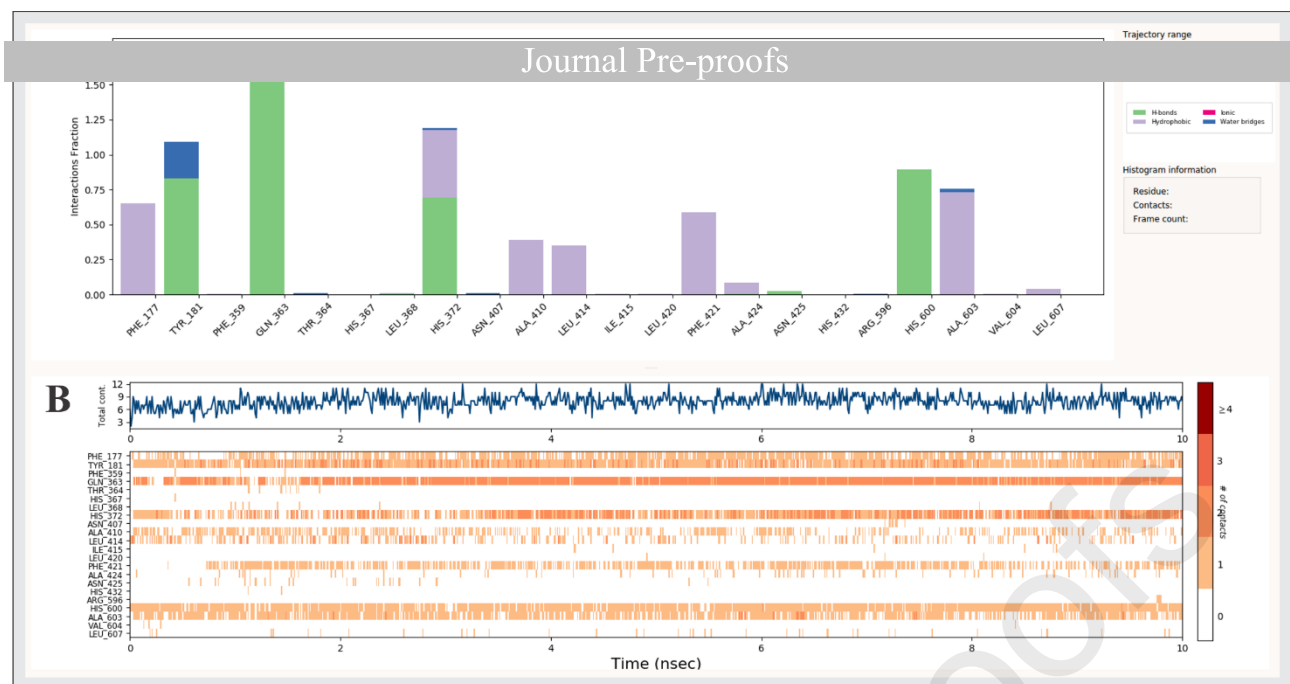


Fig. 11. Normalized stacked bar chart representation and timeline representation of interactions and contacts between 5-LO enzyme and compound **19** during the course of 10 ns molecular dynamics simulation.

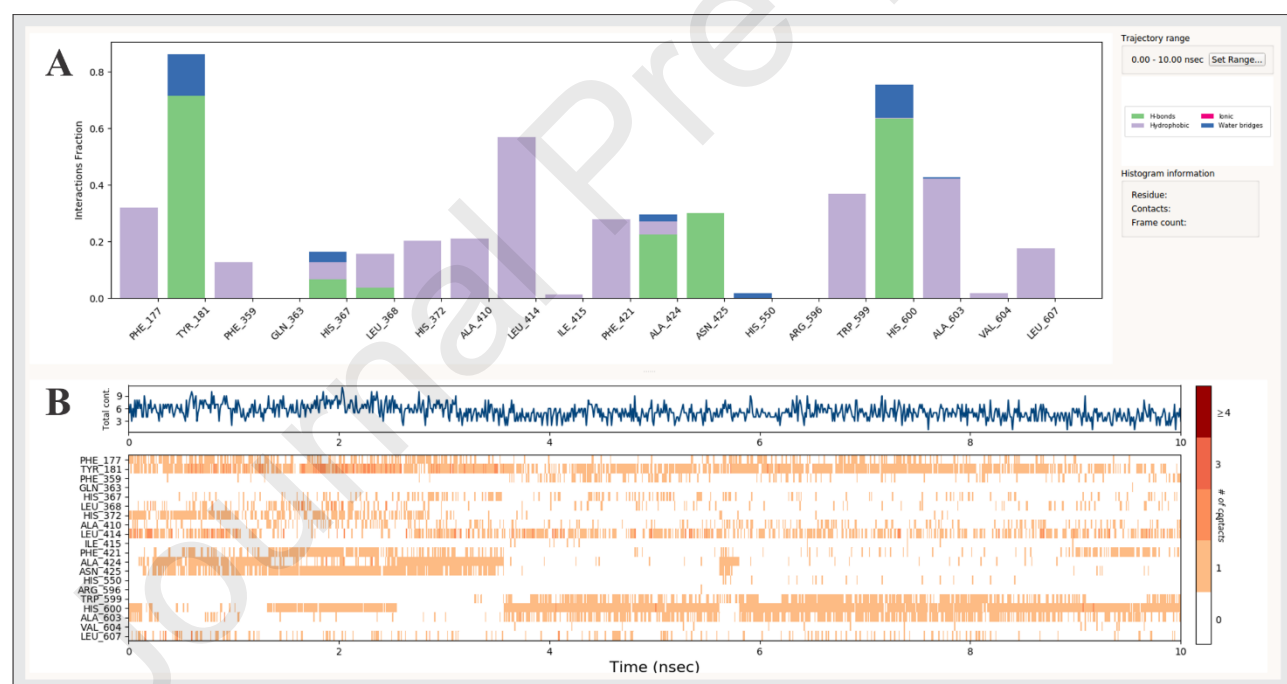


Fig. 12. Normalized stacked bar chart representation and timeline representation of interactions and contacts between 5-LO enzyme and compound **20** during the course of 10 ns molecular dynamics simulation.

3.3. *In silico* study of the physico-chemical, pharmacokinetic and toxicological properties

Journal Pre-proofs

Previously, we found that compound **18** showed no cytotoxic effects at concentration of 10 μM [36]. In order to obtain a more complete picture of the most potent DNase I inhibitors (**18-20**) within the studied compounds, their physico-chemical properties were calculated using Molinspiration tool [39] (Table S8). According to the results, the three most active compounds (**18-20**) fulfilled Lipinski's rule of five and therefore were predicted to have good oral bioavailability [57–59]. Additionally, all three compounds (**18-20**), as promising leads in the treatment of Alzheimer's disease, fulfilled all the requirements necessary for a compound to be predicted as a successful CNS drug ($m_i\text{LogP} < 5$, $\text{TPSA} < 60\text{-}70 \text{ \AA}^2$, $n_{\text{ON}} < 7$, $n_{\text{OHNH}} < 3$, $n_{\text{rotb}} < 8$, and $\text{MW} < 450$) [60] (Table S8). Prediction performed by admetSAR [40] confirms that compounds **18-20** might be able to pass through blood-brain barrier (BBB) and penetrate into the CNS. Considering toxicological properties calculated by DataWarrior [41], compounds **18-20** were predicted with no risk for mutagenic, tumorigenic, reproductive or irritant effects.

4. CONCLUSION

A series of twenty 4-(4-chlorophenyl)thiazol-2-amines was tested on DNase I inhibition *in vitro*. Three compounds (**18-20**) inhibited DNase I with IC_{50} value below 100 μM , being more potent than crystal violet, used as a positive control. A computational approach has been exploited to reveal the relationship between the DNase I inhibitory activity and the pharmacophore features found in the 4-(4-chlorophenyl)thiazol-2-amines. Also, compounds **18-20** have been shown as very potent 5-LO inhibitors with nanomolar IC_{50} values obtained in cell-free assay, with compound **20** as the most potent ($\text{IC}_{50} = 50 \text{ nM}$). Molecular docking and molecular dynamics simulations defined the 4-(4-chlorophenyl)thiazol-2-amines interactions with the most important residues of DNase I and 5-LO.

Based on our *in silico* study, compounds **18-20** were predicted to have good oral bioavailability, might be able to pass through BBB and penetrate into the CNS, and were also predicted as compounds with no toxic effects. Thiazol-2-amines can be regarded as a promising scaffold for design of new DNase I inhibitors and could have potential therapeutic applications due to the significant involvement of DNase I in pathophysiology of many disease conditions. Compounds **18-20** could be set as a good starting point for the development of novel dual inhibitors of 5-LO and DNase I, enzymes involved in the development of neurodegenerative disorders among elderly, including Alzheimer's disease. Worth mentioning at this point is that 5-LO activity is not essential for DNase I inhibition as also compounds **1**, **7-10** and **14-17** are very potent 5-LO inhibitors [35,36] but show very different activities towards DNase I.

CONFLICT OF INTEREST

ACKNOWLEDGMENTS

We thank Dr. D. Vogt, Dr. S. Woltersdorf and Dr. S. Barzen for synthesis and Dr. S. Kretschmer for measurement of 5-LO inhibition. The financial support of this work by Ministry of Education, Science and Technological Development of the Republic of Serbia (Grants No. OI 172044 and OI 171025) and Faculty of Medicine of the University of Niš (Internal project No. 4) as well as the EU COST Action 13135 is gratefully acknowledged. The authors would like to thank Schrödinger LLC for providing us the academic licenses free of cost for this study, and the Alexander von Humboldt Foundation, Bonn, Germany, for financial support of the visit of H. S. to A. S. in Serbia. Additional travel funding is acknowledged by HHU Funds for International Relationships (A. Z.).

REFERENCES

- [1] D. Smokawa, S.I. Tanuma, Characterization of human DNase I family endonucleases and activation of DNase γ during apoptosis, *Biochemistry* 40 (2001) 143–152.
- [2] K. Samejima, W.C. Earnshaw, Trashing the genome: the role of nucleases during apoptosis, *Nat. Rev. Mol. Cell Biol.* 6 (2005) 677–688.
- [3] H.M. Eun, Nucleases, in: *Enzymology primer for recombinant DNA technology*, Elsevier, 1996; pp. 145–232.
- [4] B. Polzar, M.C. Peitsch, R. Loos, J. Tschopp, H.G. Mannherz, Overexpression of deoxyribonuclease I (DNase I) transfected into COS-cells: its distribution during apoptotic cell death, *Eur. J. Cell Biol.* 62 (1993) 397–405.
- [5] M.C. Peitsch, B. Polzar, H. Stephan, T. Crompton, H.R. MacDonald, H.G. Mannherz, J. Tschopp, Characterization of the endogenous deoxyribonuclease involved in nuclear DNA degradation during apoptosis (programmed cell death), *EMBO J.* 12 (1993) 371–377.
- [6] F. Rauch, B. Polzar, H. Stephan, S. Zanotti, R. Paddenberg, H.G. Mannherz, Androgen ablation leads to an upregulation and intranuclear accumulation of deoxyribonuclease I in rat prostate epithelial cells paralleling their apoptotic elimination, *J. Cell Biol.* 137 (1997) 909–923.
- [7] M. Oliveri, A. Daga, C. Cantoni, C. Lunardi, R. Millo, A. Puccetti, DNase I mediates internucleosomal DNA degradation in human cells undergoing drug-induced apoptosis, *Eur. J. Immunol.* 31 (2001) 743–751.
- [8] M. Oliveri, A. Daga, C. Lunardi, R. Navone, R. Millo, A. Puccetti, DNase I behaves as a transcription factor which modulates Fas expression in human cells, *Eur. J. Immunol.* 34 (2004) 273–279.
- [9] D. Eulitz, H.G. Mannherz, Inhibition of deoxyribonuclease I by actin is to protect cells from premature cell death, *Apoptosis* 12 (2007) 1511–1521.
- [10] S. Elmore, Apoptosis: a review of programmed cell death, *Toxicol. Pathol.* 35 (2007) 495–516.
- [11] O. Isacson, On neuronal health, *Trends Neurosci.* 16 (1993) 306–308.
- [12] N. Heintz, Cell death and the cell cycle: a relationship between transformation and neurodegeneration? *Trends Biochem. Sci.* 18 (1993) 157–159.
- [13] C.B. Thompson, Apoptosis in the pathogenesis and treatment of disease, *Science* 267 (1995) 1456–1462.
- [14] M. Tanaka, H. Ito, S. Adachi, H. Akimoto, T. Nishikawa, T. Kasajima, F. Marumo, M. Hiroe, Hypoxia induces apoptosis with enhanced expression of Fas antigen messenger RNA in cultured neonatal rat cardiomyocytes, *Circ. Res.* 75 (1994) 426–433.

- [15] D.M. Rosenbaum, J. Kalberg, J.A. Kessler, Superoxide dismutase ameliorates neuronal death from hypoxia in culture, *Stroke* 25 (1994) 857–862.
- [16] R.D. Goldin, N.C. Hunt, J. Clark, S.N. Wickramasinghe, Apoptotic bodies in a murine model of alcoholic liver disease: Reversibility of ethanol-induced changes, *J. Pathol.* 171 (1993) 73–76.
- [17] J.A. Nitahara, W. Cheng, Y. Liu, B. Li, A. Leri, P. Li, D. Mogul, S.R. Gambert, J. Kajstura, P. Anversa, Intracellular calcium, DNase activity and myocyte apoptosis in aging Fischer 344 rats, *J. Mol. Cell. Cardiol.* 30 (1998) 519–535.
- [18] M. Yao, A. Keogh, P. Spratt, C.G. dos Remedios, P.C. Kieβling, Elevated DNase I levels in human idiopathic dilated cardiomyopathy: an indicator of apoptosis? *J. Mol. Cell. Cardiol.* 28 (1996) 95–101.
- [19] B. Zhu, Y. Gong, P. Chen, H. Zhang, T. Zhao, P. Li, Increased DNase I activity in diabetes might be associated with injury of pancreas, *Mol. Cell. Biochem.* 393 (2014) 23–32.
- [20] M. Takeda, K. Fukuoka, H. Endou, Cisplatin-induced apoptosis in mouse proximal tubular cell line, in: H. Koide, I. Ichikawa (Eds.), *Progression of Chronic Renal Diseases, Contrib Nephrol. Basel, Karger* 118 (1996) 24–28.
- [21] A.G. Basnakian, E.O. Apostolov, X. Yin, M. Napirei, H.G. Mannherz, S.V. Shah, Cisplatin nephrotoxicity is mediated by deoxyribonuclease I, *J. Am. Soc. Nephrol.* 16 (2005) 697–702.
- [22] X. Yin, E.O. Apostolov, S.V. Shah, X. Wang, K.V. Bogdanov, T. Buzder, A.G. Stewart, A.G. Basnakian, Induction of renal endonuclease G by cisplatin is reduced in DNase I-deficient mice, *J. Am. Soc. Nephrol.* 18 (2007) 2544–2553.
- [23] E.O. Apostolov, I. Soultanova, A. Savenka, O.O. Bagandov, X. Yin, A.G. Stewart, R.B. Walker, A.G. Basnakian, Deoxyribonuclease I is essential for DNA fragmentation induced by gamma radiation in mice, *Radiat. Res.* 172 (2009) 481–492.
- [24] M. Napirei, A.G. Basnakian, E.O. Apostolov, H.G. Mannherz, Deoxyribonuclease 1 aggravates acetaminophen-induced liver necrosis in male CD-1 mice, *Hepatology* 43 (2006) 297–305.
- [25] M.E. Khalifa, Recent developments and biological activities of 2-aminothiazole derivatives, *Acta Chim. Slov.* 65 (2018) 1–22.
- [26] D. Das, P. Sikdar, M. Bairagi, Recent developments of 2-aminothiazoles in medicinal chemistry, *Eur. J. Med. Chem.* 109 (2016) 89–98.
- [27] A. Kolarevic, D. Yancheva, G. Kocic, A. Smelcerovic, Deoxyribonuclease inhibitors, *Eur. J. Med. Chem.* 88 (2014) 101–111.

- [28] B.S. Ilić, A. Kolarević, G. Kocić, A. Šmelcerović, Ascorbic acid as DNase I inhibitor in prevention of male infertility, *Biochem. Biophys. Res. Commun.* 498 (2018) 1075–1077.
- [29] A. Kolarević, B.S. Ilić, N. Anastassova, A.T. Mavrova, D. Yancheva, G. Kocić, A. Šmelcerović, Benzimidazoles as novel deoxyribonuclease I inhibitors, *J. Cell. Biochem.* 119 (2018) 8937–8948.
- [30] A.T. Mavrova, S. Dimov, D. Yancheva, A. Kolarević, B.S. Ilić, G. Kocić, A. Šmelcerović, Synthesis and DNase I inhibitory properties of some 5,6,7,8-tetrahydrobenzo[4,5]thieno[2,3-*d*]pyrimidines, *Bioorg. Chem.* 80 (2018) 693–705.
- [31] A. Kolarević, B.S. Ilić, G. Kocić, Z. Džambaski, A. Šmelcerović, B.P. Bondžić, Synthesis and DNase I inhibitory properties of some 4-thiazolidinone derivatives, *J. Cell. Biochem.* 120 (2019) 264–274.
- [32] A. Kolarevic, A. Pavlovic, A. Djordjevic, J. Lazarevic, S. Savic, G. Kocic, M. Anderluh, A. Smelcerovic, Rutin as deoxyribonuclease I inhibitor, *Chem. Biodivers.* 16 (2019) e1900069.
- [33] B.P. Bondžić, Z. Džambaski, A. Kolarević, A. Đorđević, M. Anderluh, A. Šmelcerović, Synthesis and DNase I inhibitory properties of new benzocyclobutane-2,5-diones, *Future Med. Chem.* 11 (2019) 2415–2426.
- [34] C.B. Rödl, D. Vogt, S.B. Kretschmer, K. Ihlefeld, S. Barzen, A. Brüggerhoff, J. Achenbach, E. Proschak, D. Steinhilber, H. Stark, B. Hofmann, Multi-dimensional target profiling of *N*,4-diaryl-1,3-thiazole-2-amines as potent inhibitors of eicosanoid metabolism, *Eur. J. Med. Chem.* 84 (2014) 302–311.
- [35] D. Vogt, J. Weber, K. Ihlefeld, A. Brüggerhoff, E. Proschak, H. Stark, Design, synthesis and evaluation of 2-aminothiazole derivatives as sphingosine kinase inhibitors, *Bioorg. Med. Chem.* 22 (2014) 5354–5367.
- [36] S.B.M. Kretschmer, S. Woltersdorf, C.B. Rödl, D. Vogt, A.K. Häfner, D. Steinhilber, H. Stark, B. Hofmann, Development of novel aminothiazole-comprising 5-LO inhibitors, *Future Med. Chem.* 8 (2016) 149–164.
- [37] Small-Molecule Drug Discovery Suite 2015-1, Schrödinger, LLC, New York, NY, 2015.
- [38] S.L. Dixon, A.M. Smondyrev, E.H. Knoll, S.N. Rao, D.E. Shaw, R.A. Friesner, PHASE: A new engine for pharmacophore perception, 3D QSAR model development, and 3D database screening: 1. Methodology and preliminary results, *J. Comput. Aided Mol. Des.* 20 (2006) 647–671.
- [39] Molinspiration Cheminformatics. <http://www.molinspiration.com/> (accessed September 2018)
- [40] admetSAR. <http://lmmd.ecust.edu.cn/admetsar1/> (accessed April 2019)
- [41] DataWarrior. <http://www.openmolecules.org/datawarrior/> (accessed April 2019)

- [42] S.J. Jones, A.F. Worrall, B.A. Connolly, Site-directed mutagenesis of the catalytic residues of bovine pancreatic deoxyribonuclease I, *J. Mol. Biol.* 204 (1996) 1154–1163.
- [43] M. Guérout, D. Picot, J. Abi-Ghanem, B. Hartmann, M. Baaden, How cations can assist DNase I in DNA binding and hydrolysis, *PLoS Comput. Biol.* 6 (2010) e1001000, 1–11.
- [44] C.Q. Pan, J.S. Ulmer, A. Herzka, R.A. Lazarus, Mutational analysis of human DNase I at the DNA binding interface: Implications for DNA recognition, catalysis, and metal ion dependence, *Protein Sci.* 7 (1998) 628–636.
- [45] H. Manev, T. Uz, K. Sugaya, T. Qu, Putative role of neuronal 5-lipoxygenase in an aging brain, *FASEB J.* 14 (2000) 1464–1469.
- [46] J. Chu, D. Praticò, The 5-lipoxygenase as a common pathway for pathological brain and vascular aging, *Cardiovasc. Psychiatry Neurol.* 2009 (2009) 1–5.
- [47] C. Pergola, O. Werz, 5-Lipoxygenase inhibitors: a review of recent developments and patents, *Expert Opin. Ther. Pat.* 20 (2010) 355–375.
- [48] D. Steinhilber, B. Hofmann, Recent advances in the search for novel 5-lipoxygenase inhibitors, *Basic Clin. Pharmacol. Toxicol.* 114 (2014) 70–77.
- [49] C.M. Chinnici, Y. Yao, D. Praticò, The 5-lipoxygenase enzymatic pathway in the mouse brain: young versus old, *Neurobiol. Aging* 28 (2007) 1457–1462.
- [50] O. Firuzi, J. Zhuo, C.M. Chinnici, T. Wisniewski, D. Praticò, 5-Lipoxygenase gene disruption reduces amyloid- β pathology in a mouse model of Alzheimer's disease, *FASEB J.* 22 (2008) 1169–1178.
- [51] M.D. Ikonovic, E.E. Abrahamson, T. Uz, H. Manev, S.T. DeKosky, Increased 5-lipoxygenase immunoreactivity in the hippocampus of patients with Alzheimer's disease, *J. Histochem. Cytochem.* 56 (2008) 1065–1073.
- [52] Y.B. Joshi, D. Praticò, The 5-lipoxygenase pathway: oxidative and inflammatory contributions to the Alzheimer's disease phenotype, *Front. Cell. Neurosci.* 8 (2015) 436.
- [53] Y. Higami, I. Shimokawa, Apoptosis in the aging process, *Cell Tissue Res.* 301 (2000) 125–132.
- [54] T. Halgren, New method for fast and accurate binding-site identification and analysis, *Chem. Biol. Drug Des.* 69 (2007) 146–148.
- [55] S. Ishii, M. Noguchi, M. Miyano, T. Matsumoto, M. Noma, Mutagenesis studies on the amino acid residues involved in the iron-binding and the activity of human 5-lipoxygenase, *Biochem. Biophys. Res. Commun.* 182 (1992) 1482–1490.
- [56] N.C. Gilbert, S.G. Bartlett, M.T. Waight, D.B. Neau, W.E. Boeglin, A.R. Brash, M.E. Newcomer, The structure of human 5-lipoxygenase, *Science* 331 (2011) 217–219.

- [57] C.A. Lipinski, F. Lombardo, B.W. Dominy, P.J. Feeney, Experimental and computational approaches to estimate solubility and permeability in drug discovery and development settings, *Adv. Drug Deliv. Rev.* 64 (2012) 4–17.
- [58] P. Ertl, B. Rohde, P. Selzer, Fast calculation of molecular polar surface areas as a sum of fragment-based contribution and its application to the prediction of drug transport properties, *J. Med. Chem.* 43 (2000) 3714–3717.
- [59] S. Prasanna, R.J. Doerksen, Topological polar surface area: a useful descriptor in 2D-QSAR, *Curr. Med. Chem.* 2009; 16: 21–41.
- [60] H. Pajouhesh, G.R. Lenz, Medicinal chemical properties of successful central nervous system drugs, *NeuroRx* 2 (2005) 541–553.

Supplementary tables

Table S1. RQSAR parameters for the Pharma RQSAR model.

Table S2. RQSAR parameters for the E-State RQSAR model.

Table S3. Parameters of the most important pharmacophore hypotheses.

Table S4. Inter-pharmacophoric angle measurements of the hypothesis AADHRRR.13.

Table S5. Inter-pharmacophoric site measurements of the hypothesis AADHRRR.13.

Table S6. PubChem compound dataset used for pharmacophore screening.

Table S7. Summary of the top ranked DNase I and 5-LO enzyme binding site.

Table S8. Physico-chemical properties of compounds that inhibited DNase I with IC_{50} below 200 μ M predicted by Molinspiration [39].

Supplementary figures

Fig. S1. RMSD plot of bovine pancreatic DNase I (A) and compounds **18** (B), **19** (C) and **20** (D), during the course of 10 ns molecular dynamics simulation.

Fig. S2. RMSF plot of bovine pancreatic DNase I (A) and compounds **18** (B), **19** (C) and **20** (D), during the course of 10 ns molecular dynamics simulation.

Fig. S3. RMSD plot of 5-LO enzyme (A) and compounds **18** (B), **19** (C) and **20** (D), during the course of 10 ns molecular dynamics simulation.

Fig. S4. RMSF plot of 5-LO enzyme (A) and compounds **18** (B), **19** (C) and **20** (D), during the course of 10 ns molecular dynamics simulation.

Supplementary animation contents

Animation content S1. Interactions between bovine pancreatic DNase I and compound **18** throughout the course of 10 ns molecular dynamics simulation.

Animation content S2. Interactions between bovine pancreatic DNase I and compound **19** throughout the course of 10 ns molecular dynamics simulation.

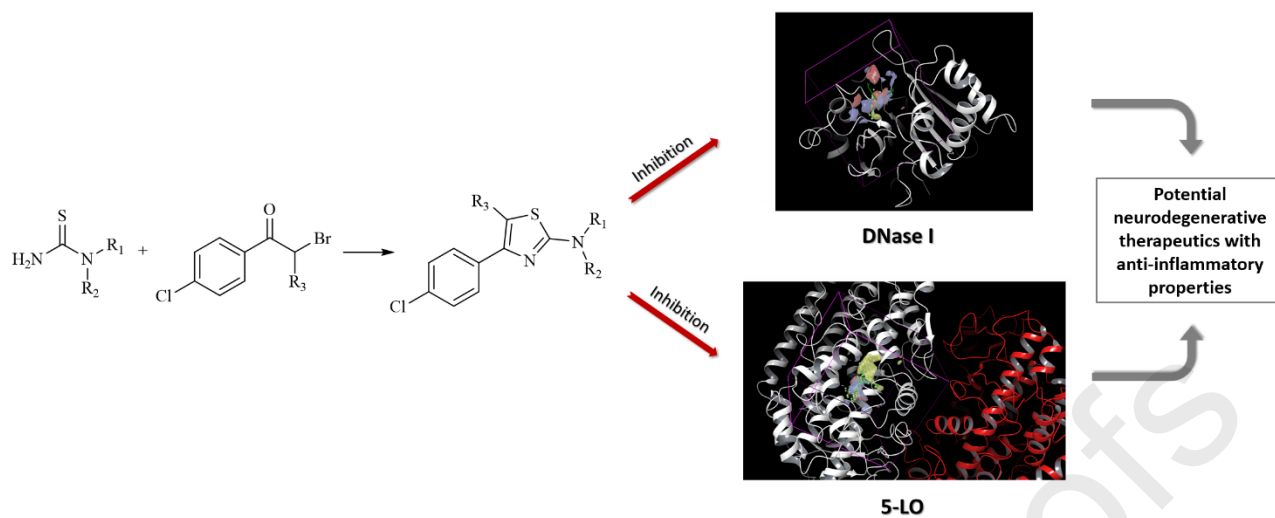
Animation content S3. Interactions between bovine pancreatic DNase I and compound **20** throughout the course of 10 ns molecular dynamics simulation.

Animation content S4. Interactions between 5-LO enzyme and compound **18** throughout the course of 10 ns molecular dynamics simulation.

Animation content S5. Interactions between 5-LO enzyme and compound **19** throughout the course of 10 ns molecular dynamics simulation.

Animation content S6. Interactions between 5-LO enzyme and compound **20** throughout the course of 10 ns molecular dynamics simulation.

Journal Pre-proofs



- Twenty 4-(4-chlorophenyl)thiazol-2-amines, of which 11 are new, were synthesized.
- Three compounds (**18-20**) inhibited DNase I with IC_{50} values below 100 μ M.
- Compounds **18-20** inhibited 5-LO with nanomolar IC_{50} values (IC_{50} for **20** was 50 nM).
- R-Group analysis, molecular docking and molecular dynamics were performed.
- Compounds **18-20** are pioneers of dual 5-LO and DNase I inhibition.

Journal Pre-proofs

Declaration of interests

Journal Pre-proofs

The authors declare that they have no known competing financial interests or personal relationships that could have appeared to influence the work reported in this paper.

The authors declare the following financial interests/personal relationships which may be considered as potential competing interests:

Journal Pre-proofs